

Title: Fundamental Physics from 21cm Cosmology

Date: Jun 02, 2008 03:40 PM

URL: <http://pirsa.org/08060032>

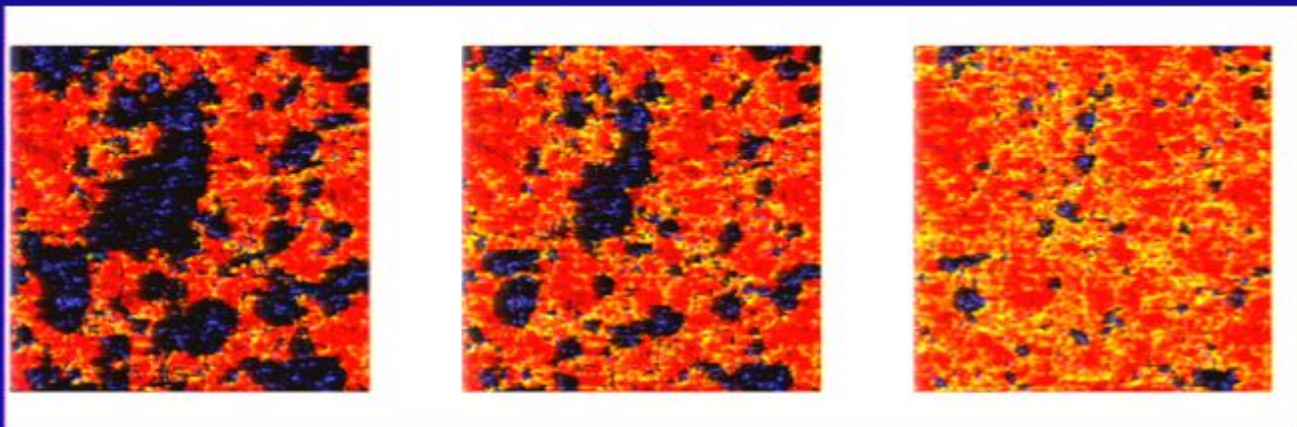
Abstract: The atomic hydrogen gas left over from the Big Bang was affected by processes ranging from quantum fluctuations during the early epoch of inflation to irradiation by the first galaxies at late times. Mapping this gas through its resonant 21cm line serves a dual role as a powerful probe of both fundamental physics and astrophysics. Current cosmological data sets (such as galaxy surveys or the microwave background) cover only 0.1% of the comoving volume of the observable Universe. 21cm observations hold the potential of mapping matter through most of the remaining volume. Radio observatories are currently being designed and constructed with this goal in mind. The three-dimensional 21cm maps could potentially set unprecedented statistical constraints on the power spectrum of cosmic density fluctuations and its gravitational growth with cosmic time. The reduced uncertainties could allow for precise measurements of fundamental parameters, such as the mass of the neutrino or the equation of state of the dark energy (from acoustic oscillations in the 21cm power spectrum), and will test generic predictions of cosmic inflation for deviations of the density fluctuations from scale invariance and gaussianity. The measured gravitational growth of the fluctuations with cosmic time would constrain the nature of the dark matter or alternative theories of gravity.

Fundamental Physics with 21cm Cosmology

Initial conditions from inflation

Nature of the dark matter and dark energy

Constrain alternative models of gravity

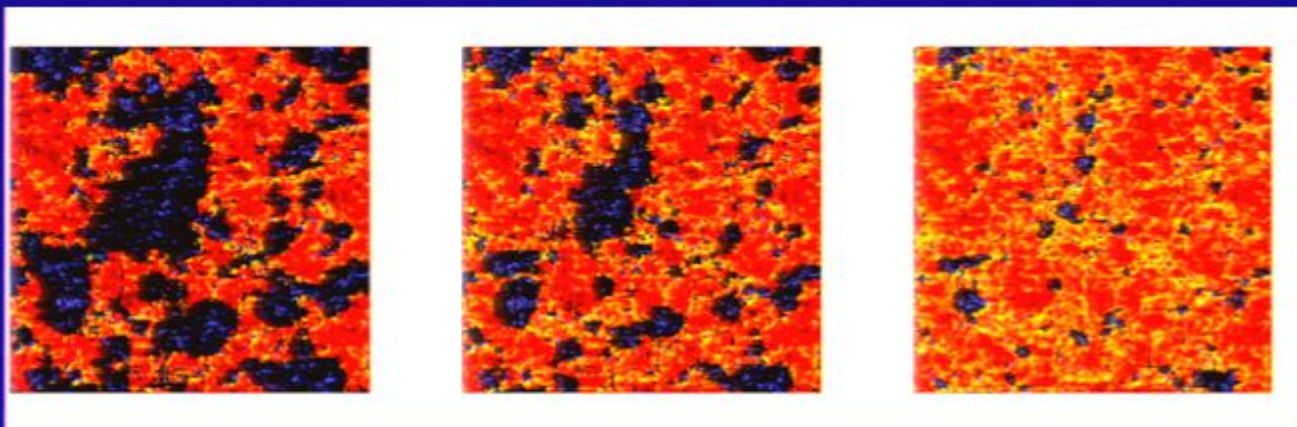


Fundamental Physics with 21cm Cosmology

Initial conditions from inflation

Nature of the dark matter and dark energy

Constrain alternative models of gravity



WMAP Cosmological Parameters

Model: Λ cdm

Data: all

$10^2 \Omega_b h^2$	$= 2.19^{+0.06}_{-0.08}$
$\ln 10^{10} A_s$	$= 0.67^{+0.04}_{-0.05}$
$\ln 10^{10} A_s$	$= 0.81^{+0.04}_{-0.05}$
$\Delta_{\mathcal{R}}^2$	$= (20 \times 10^{-10} \pm 1 \times 10^{-10}) \times 10^{-10}$
$\Delta_{\mathcal{R}}^2 (k = 0.002 / \text{Mpc})$	$= (24 \times 10^{-10} {}^{+1 \cdot 10^{-10}}_{-2 \cdot 10^{-10}}) \times 10^{-10}$
h	$= 0.71^{+0.01}_{-0.02}$
H_0	$= 71^{+1}_{-2} \text{ km s}^{-1} \text{ Mpc}^{-1}$
ℓ_A	$= 303.0^{+0.9}_{-1.3}$
n_s	$= 0.938^{+0.013}_{-0.018}$
$n_s(0.002)$	$= 0.938^{+0.012}_{-0.023}$
Ω_b	$= 0.044^{+0.002}_{-0.003}$
$\Omega_b h^2$	$= 0.0220^{+0.0006}_{-0.0008}$
Ω_c	$= 0.22^{+0.01}_{-0.02}$
Ω_Λ	$= 0.74 \pm 0.02$
Ω_m	$= 0.26^{+0.01}_{-0.03}$
$\Omega_m h^2$	$= 0.131^{+0.004}_{-0.010}$
r_s	$= 148^{+1}_{-2} \text{ Mpc}$
b_{SDSS}	$= 0.95^{+0.05}_{-0.06}$
σ_8	$= 0.75^{+0.03}_{-0.04}$
$\sigma_8 \Omega_m^{0.6}$	$= 0.34^{+0.02}_{-0.03}$
$\ln 10^{10} A_s$	$= 0.78^{+0.03}_{-0.05}$
t_0	$= 13.8^{+0.1}_{-0.2} \text{ Gyr}$
τ	$= 0.069^{+0.026}_{-0.029}$
θ_A	$= 0.594 \pm 0.002^\circ$
$\ln 10^{10} A_s$	$= 3135^{+85}_{-159}$
$\ln 10^{10} A_s$	$= 9.3^{+0.1}_{-0.0}$

The initial conditions of the Universe can be summarized on a single sheet of paper, yet thousands of books cannot fully describe the complex structures we see today...

THE DARK AGES of the Universe

Astronomers are trying to fill in
the blank pages in our photo album
of the infant universe

By Abraham Loeb

When I look up into the sky at night, I often wonder whether we humans are too preoccupied with ourselves. There is much more to the universe than meets the eye on earth. As an astrophysicist I find the privilege of being paid to think about it, and it puts things in perspective for me. There are things that I would otherwise be bothered by—my own death, for example. Everyone will die sometime, but when I see the universe as a whole, it gives me a sense of longevity. I do not care so much about myself as I would otherwise, because of the big picture.

Cosmologists are addressing some of the fundamental questions that people attempted to resolve over the centuries through philosophical thinking, but we are doing so based on systematic observation and a quantitative methodology.

Perhaps the greatest triumph of the past century has been a model of the universe that is supported by a large body of data. The value of such a model to our society is sometimes underappreciated. When I open the daily newspaper as part of my morning routine, I often see lengthy descriptions of conflicts between people about borders, possessions, or liberties. Today's news is often forgotten a few days later.

But when one opens ancient texts that have appealed to a broad audience over a longer period of time, such as the Bible, what does one often find in the opening chapter? A discussion of how the constituents of the universe—light, stars, life—were created. I

though humans are often caught up with mundane problems, they are curious about the big picture. As citizens of the universe we cannot help but wonder how the first sources of light formed, how life came into existence and whether we are alone as intelligent beings in this vast space. Astronomers in the 21st century are uniquely positioned to answer these big questions.

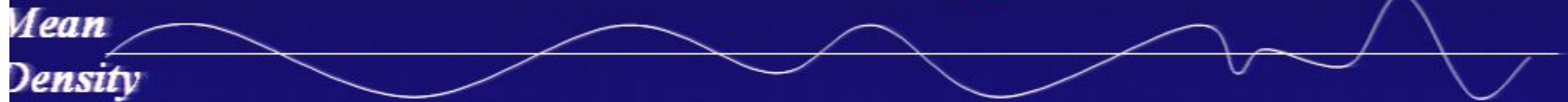
What makes modern cosmology an empirical science is that we are literally able to peer into the past. When you look at your image reflected off a mirror one meter

away, you see your image as it was one meter in the past. In cosmology, we can see the universe as it was billions of years ago.

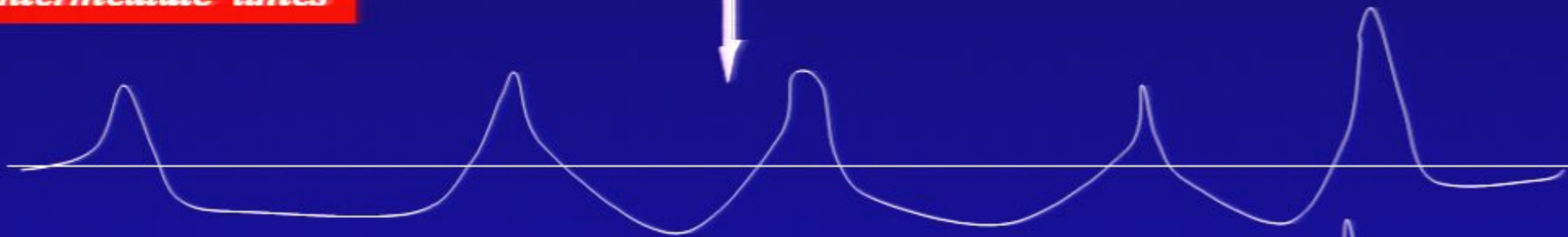
On small scales the universe is clumpy

Early times

Density perturbation

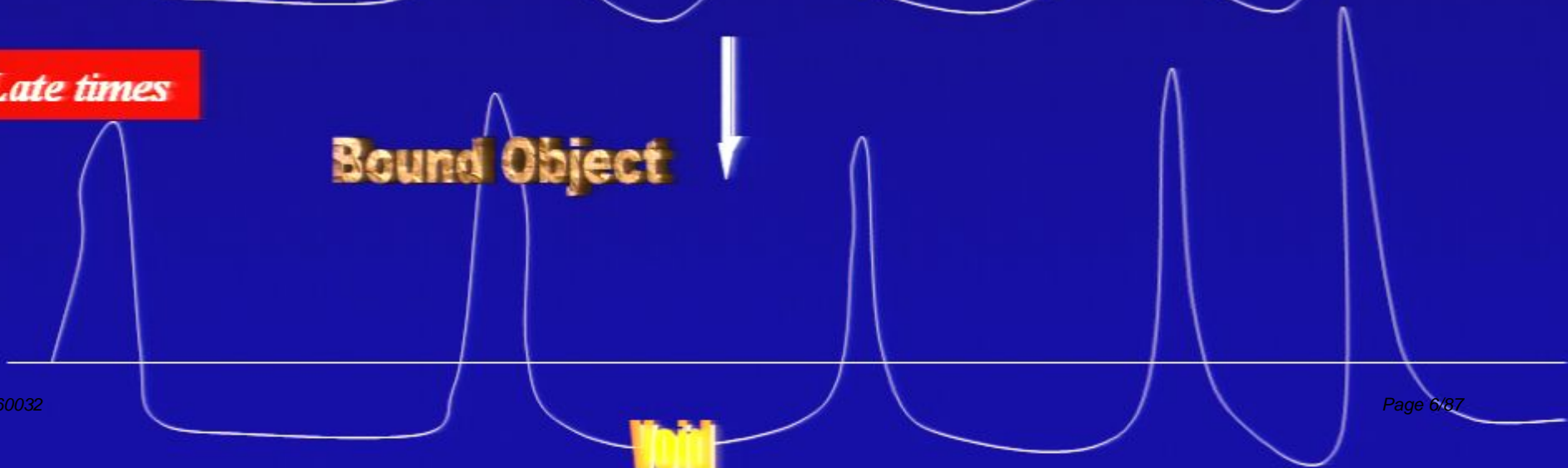


Intermediate times

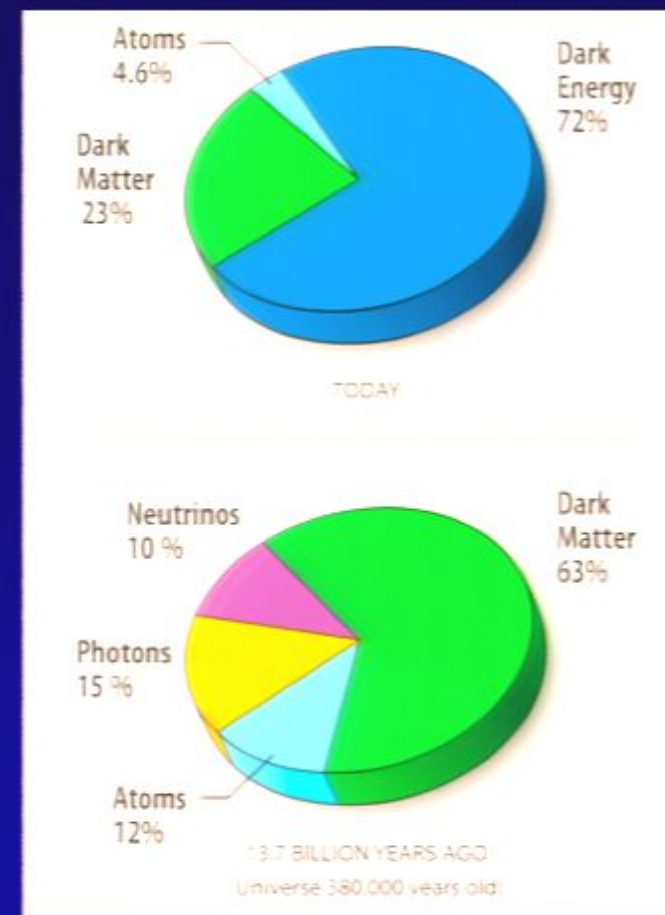
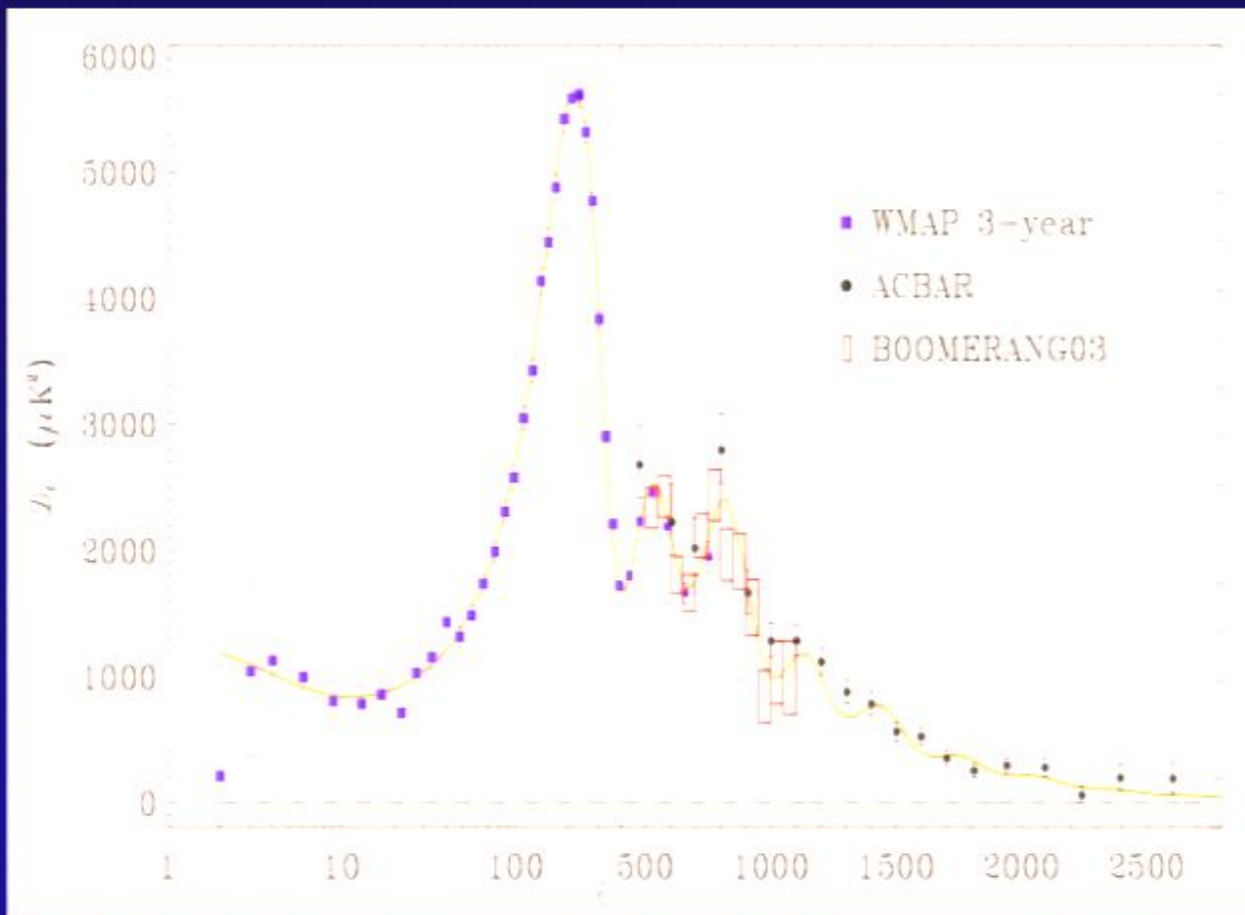


Late times

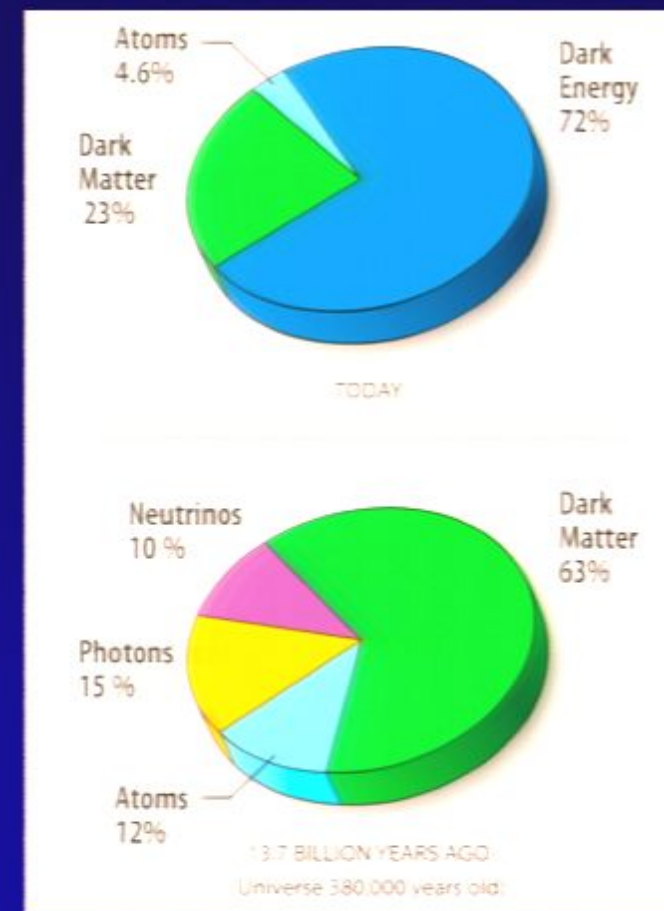
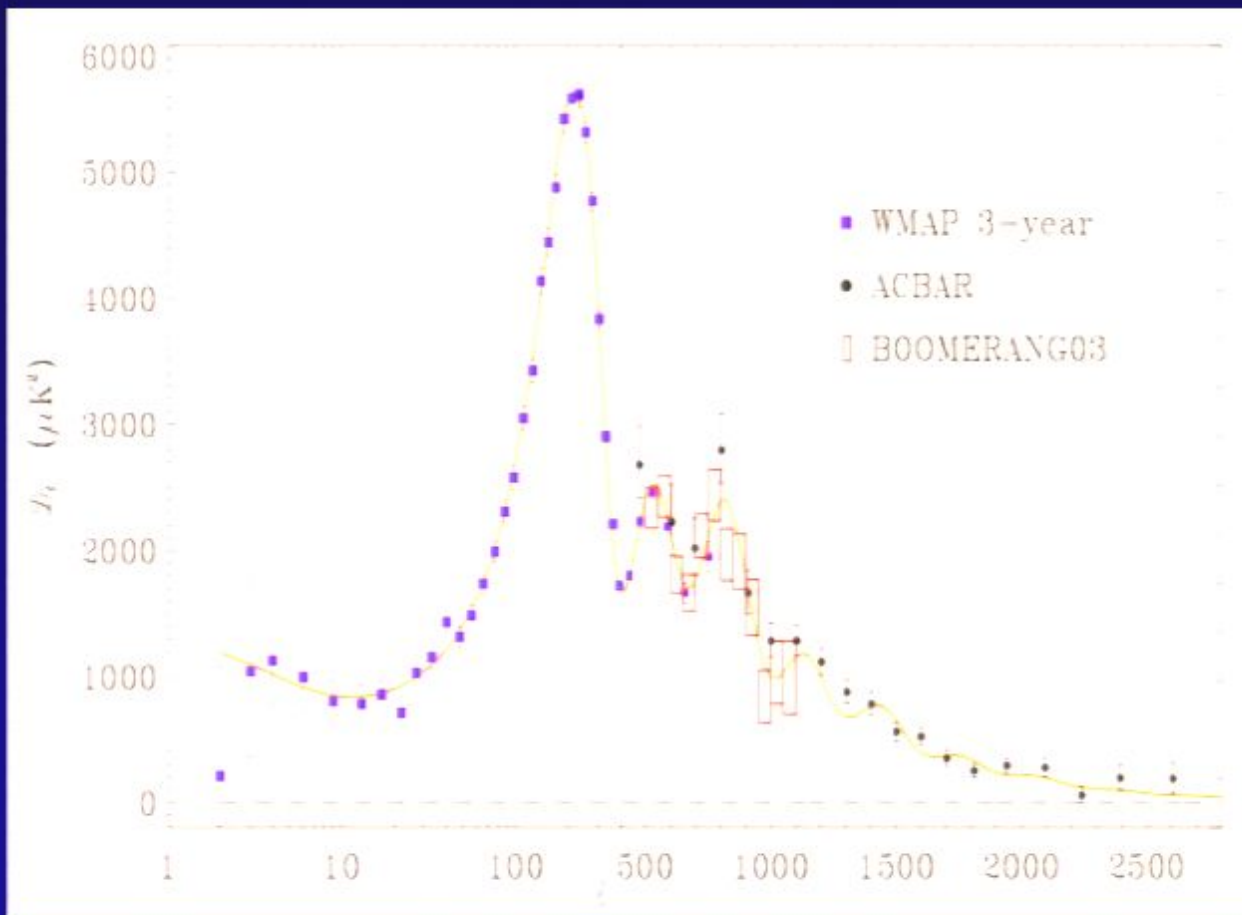
Bound Object



Evidence that Most Matter is EM Dark

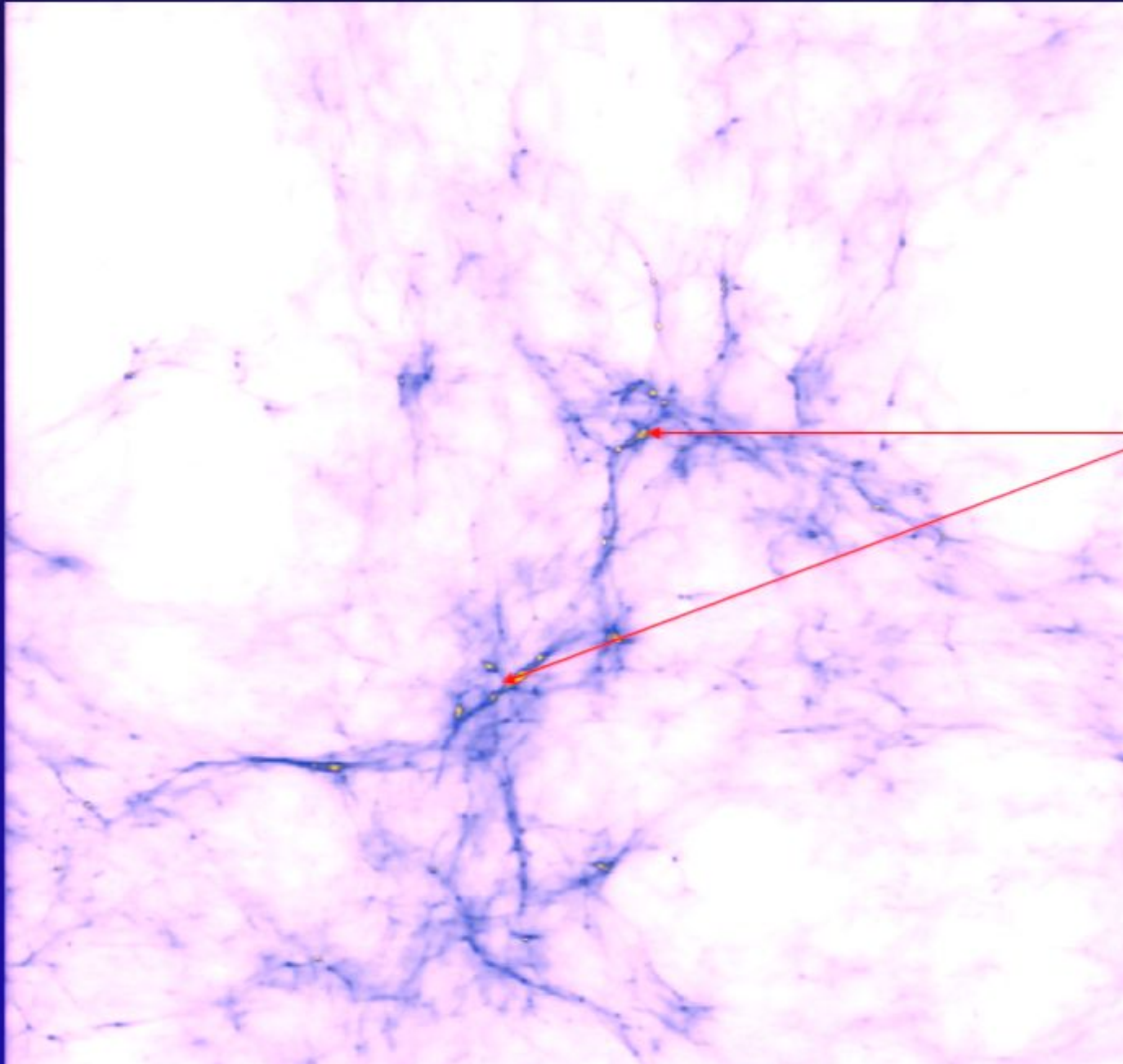


Evidence that Most Matter is EM Dark



Diffusion damping of small-scale fluctuations in the baryon-photon fluid prior to cosmic recombination implies that galaxies could not have formed in our Universe without dark matter!

The First Dwarf Galaxies Form at $z \sim 30$



*molecular
hydrogen in
Jeans mass
objects*

($\sim 10^5 M_{\odot}$)

The First Dwarf Galaxies Form at $z \sim 30$

The distribution of matter can be mapped through:

- (i) Surveys of galaxies*
- (ii) Surveys of the diffuse (intergalactic) gas*

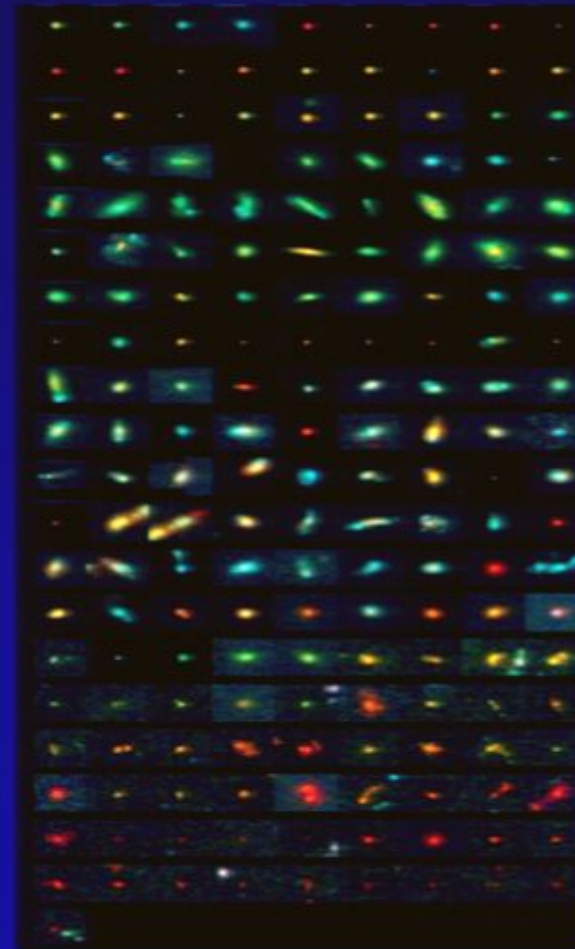
molecular hydrogen in Jeans mass objects

($\sim 10^5 M_{\odot}$)

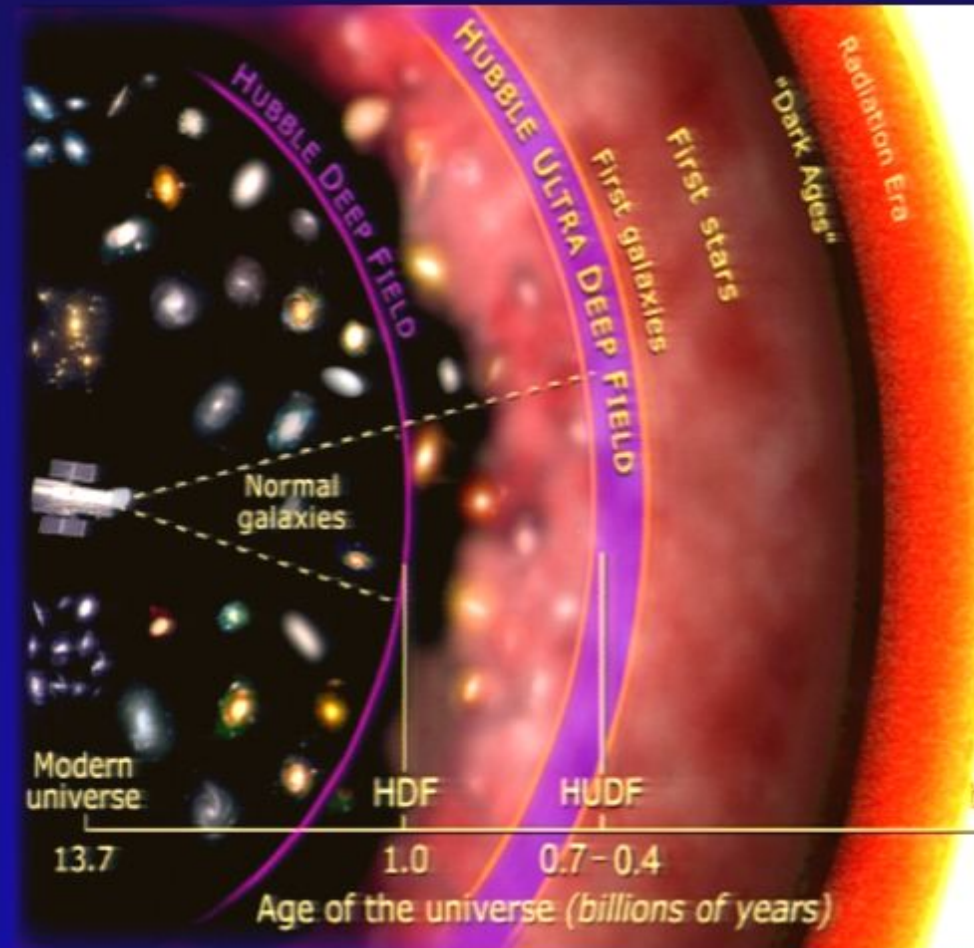
Hubble Ultra Deep Field (HUDF)

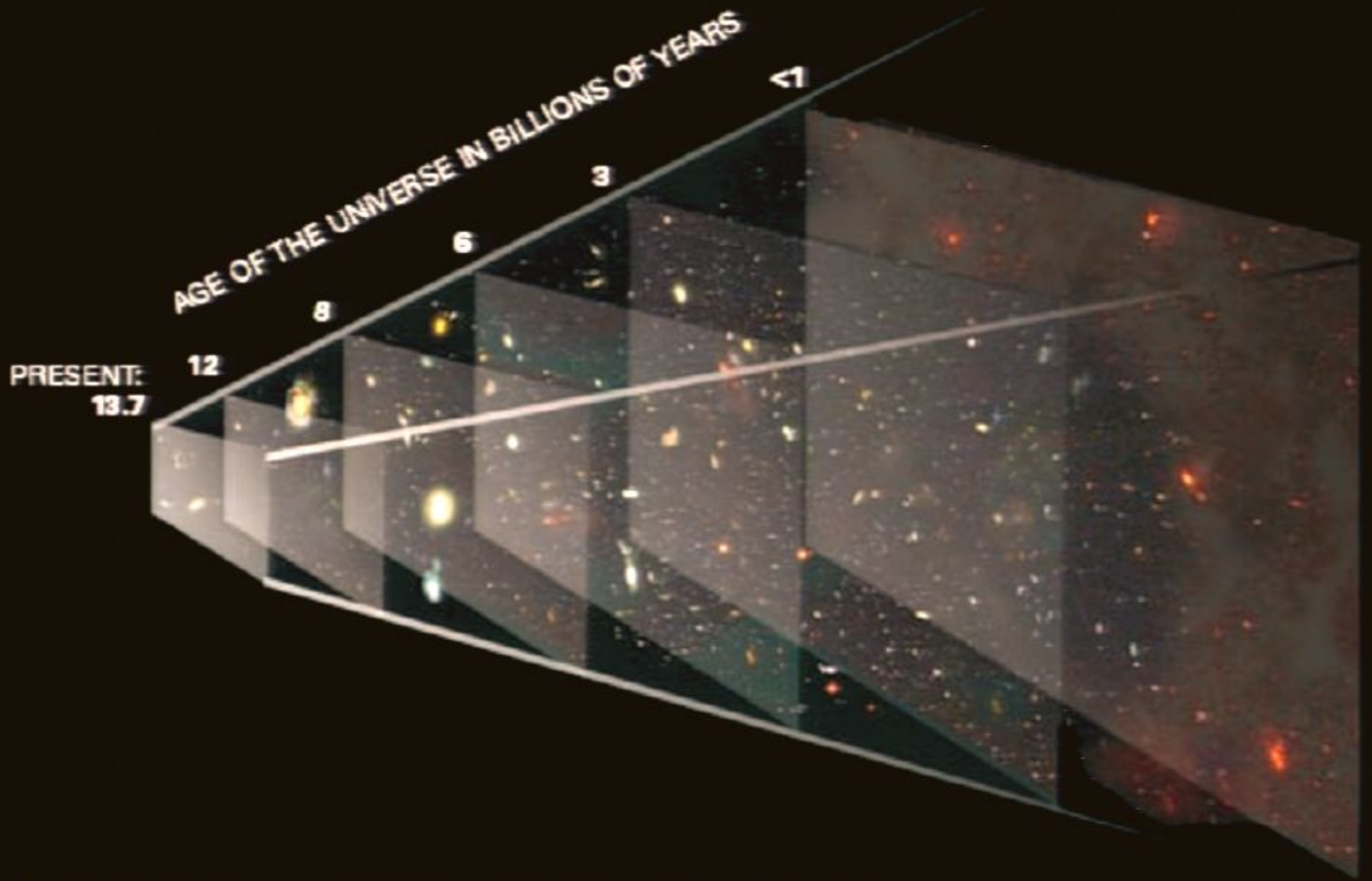


Hubble Ultra Deep Field (HUDF)



Hubble Ultra Deep Field (HUDF)



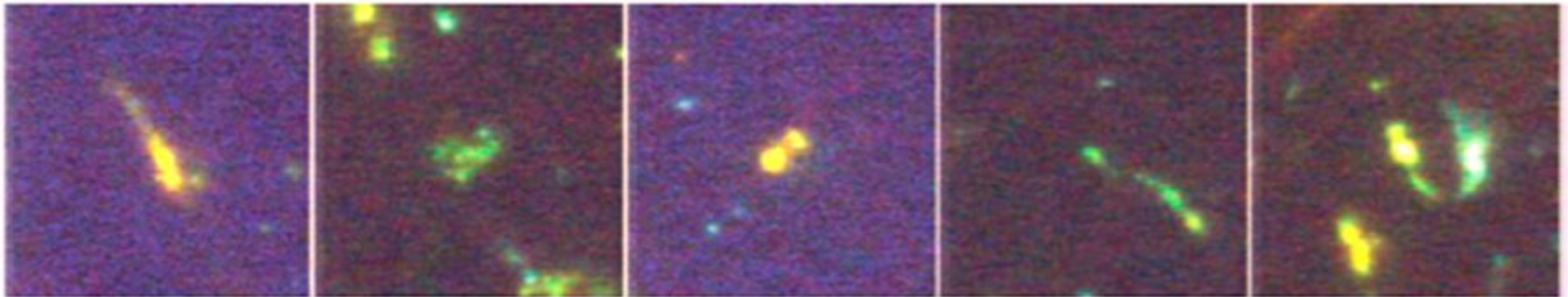


A three-dimensional view of the Hubble Ultra Deep Field. Each plane is labeled with the age of the universe at the time when the light we now see left the galaxies.

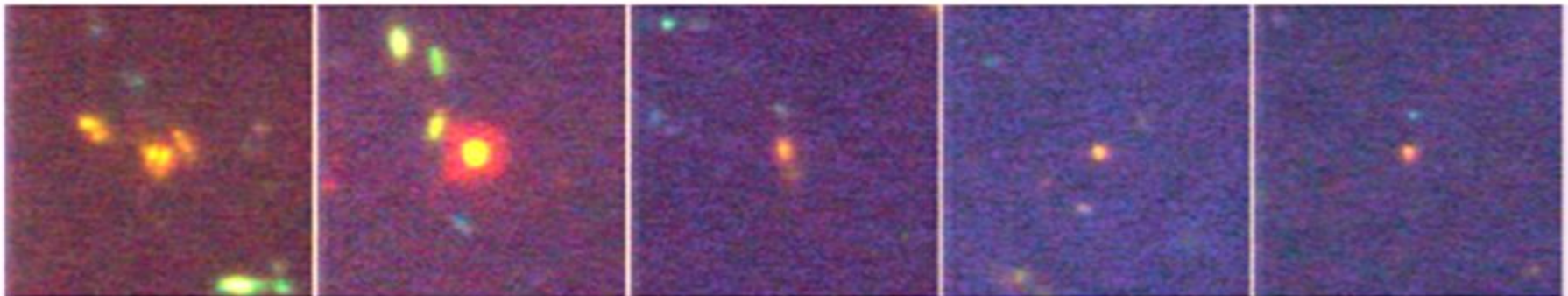
Close-up images of some of the most distant galaxies in the Hubble Ultra Deep Field

Galaxies at very early times tend to be very small and often show signs of interactions. The HUDF contains nearly 50 galaxies at redshifts 5–6, compared to a few tentative identifications in earlier, shallower observations.

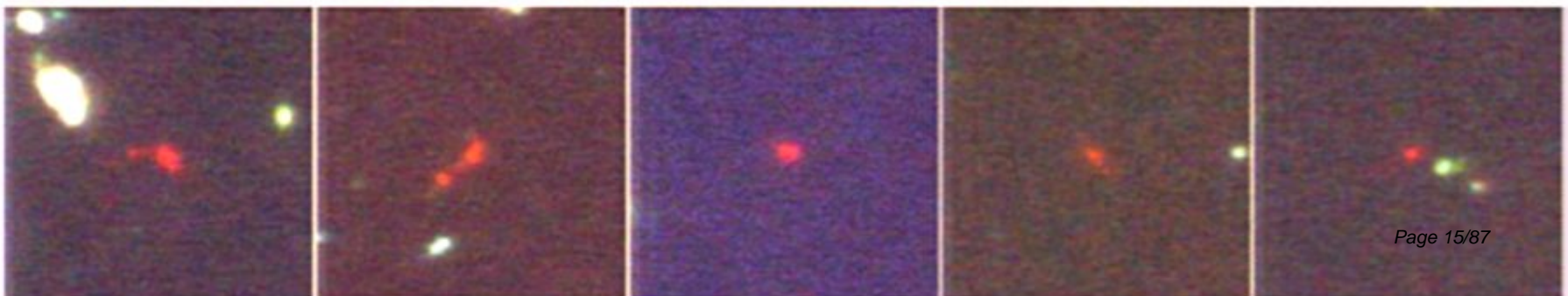
galaxies $z \sim 3\text{--}4$ Lookback time 11.4–12 billion years (312 objects)



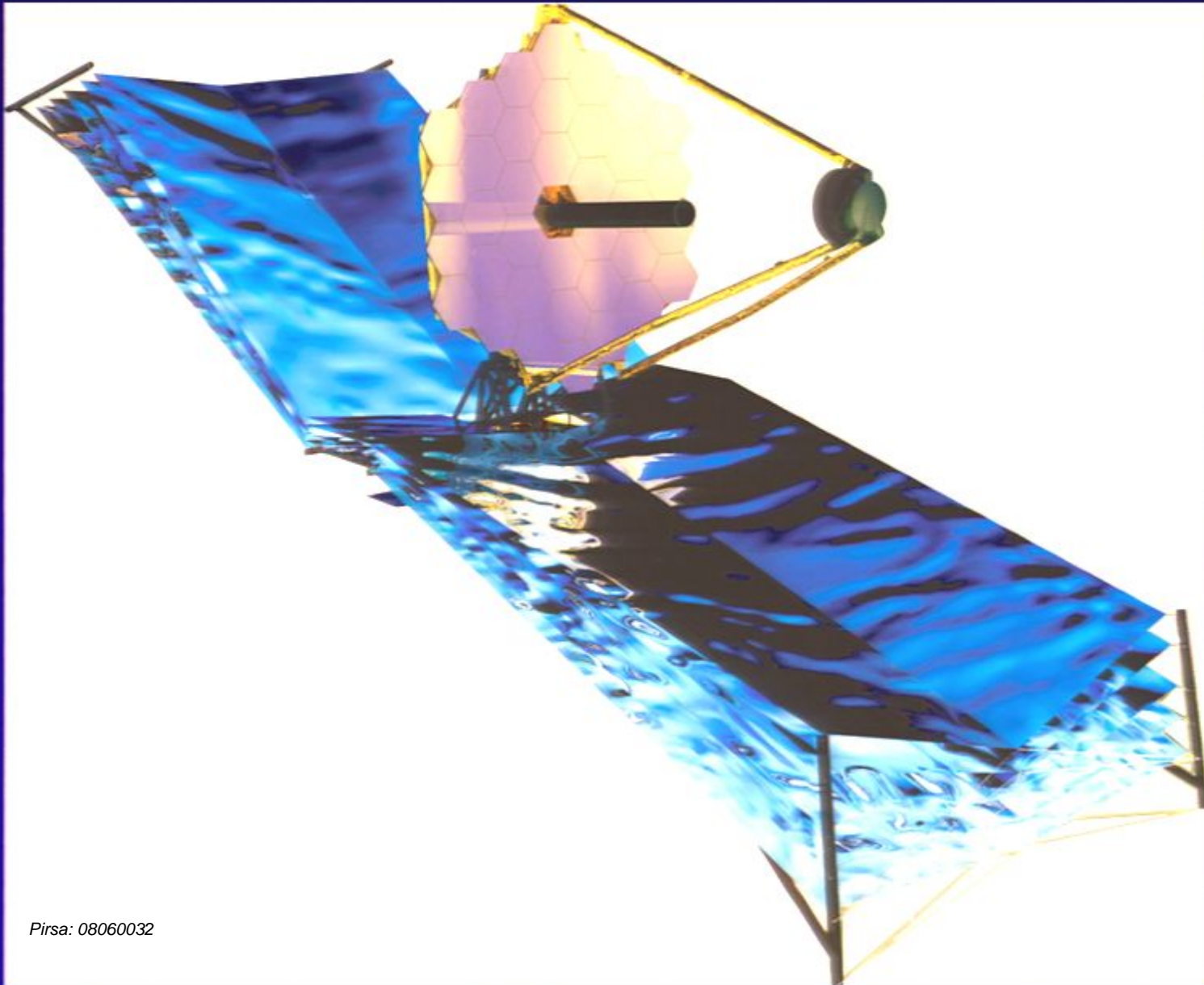
galaxies $z \sim 4\text{--}5$ Lookback time 12–12.3 billion years (79 objects)



galaxies $z > 5$ Lookback time 12.3–12.6 billion years (45 objects)



Searching for the First Galaxies: *James Webb Space Telescope*



*Mirror diameter: 6.5
meter*

Material: beryllium

18 segments

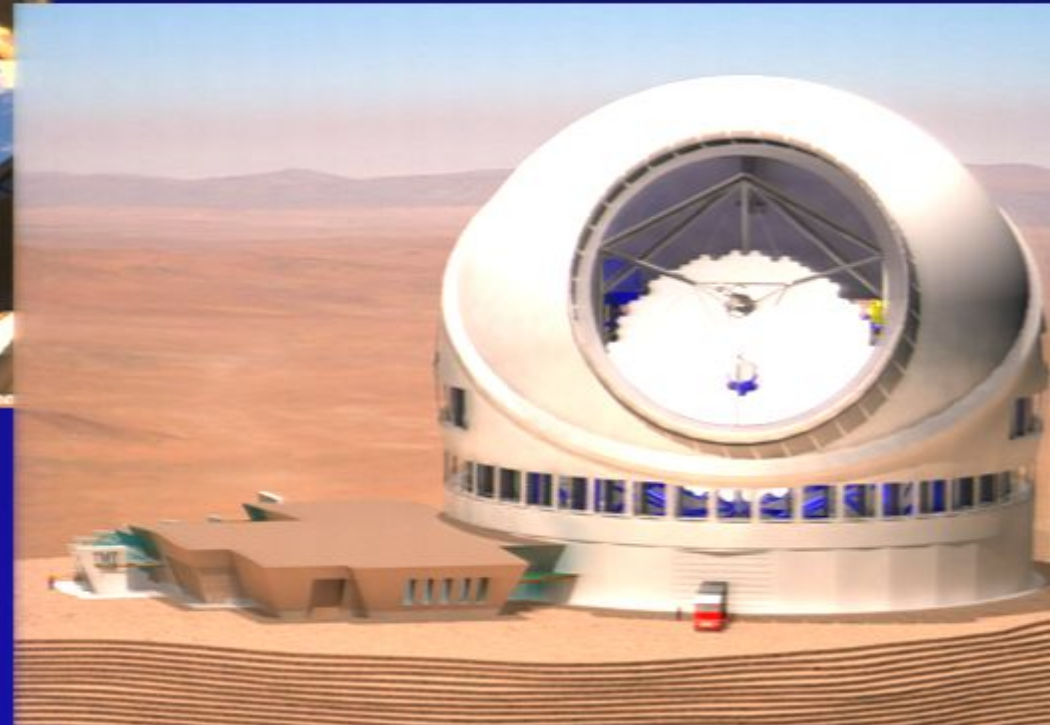
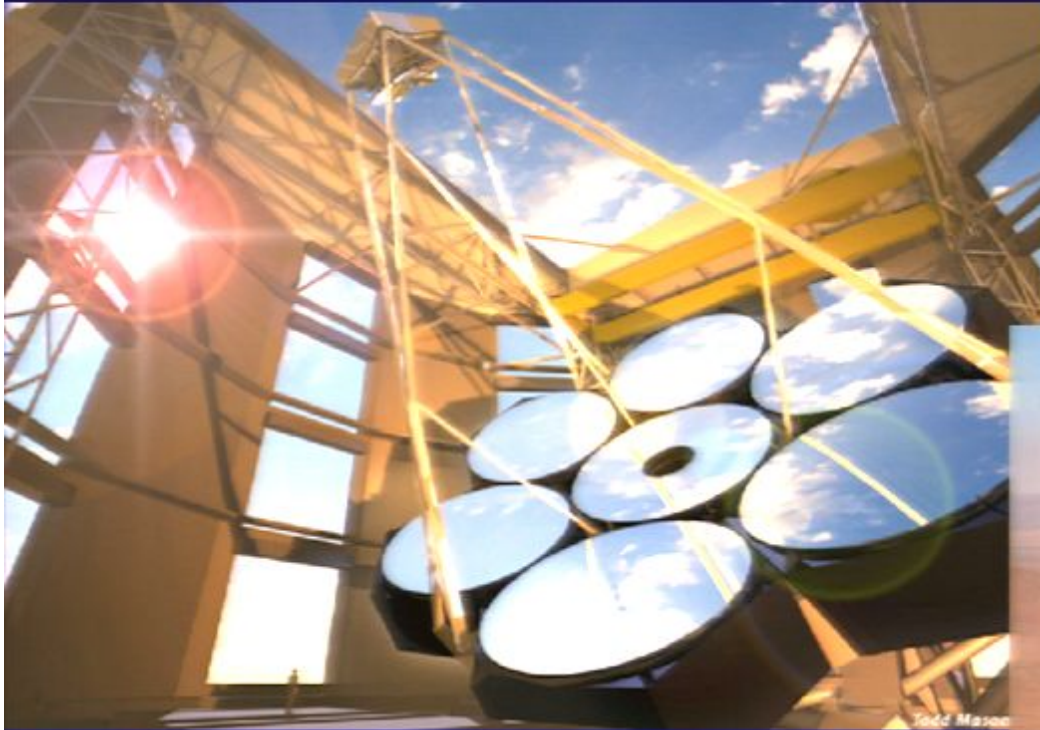
*Wavelength coverage
0.6-28 micron*

L2 orbit

~\$1 billion

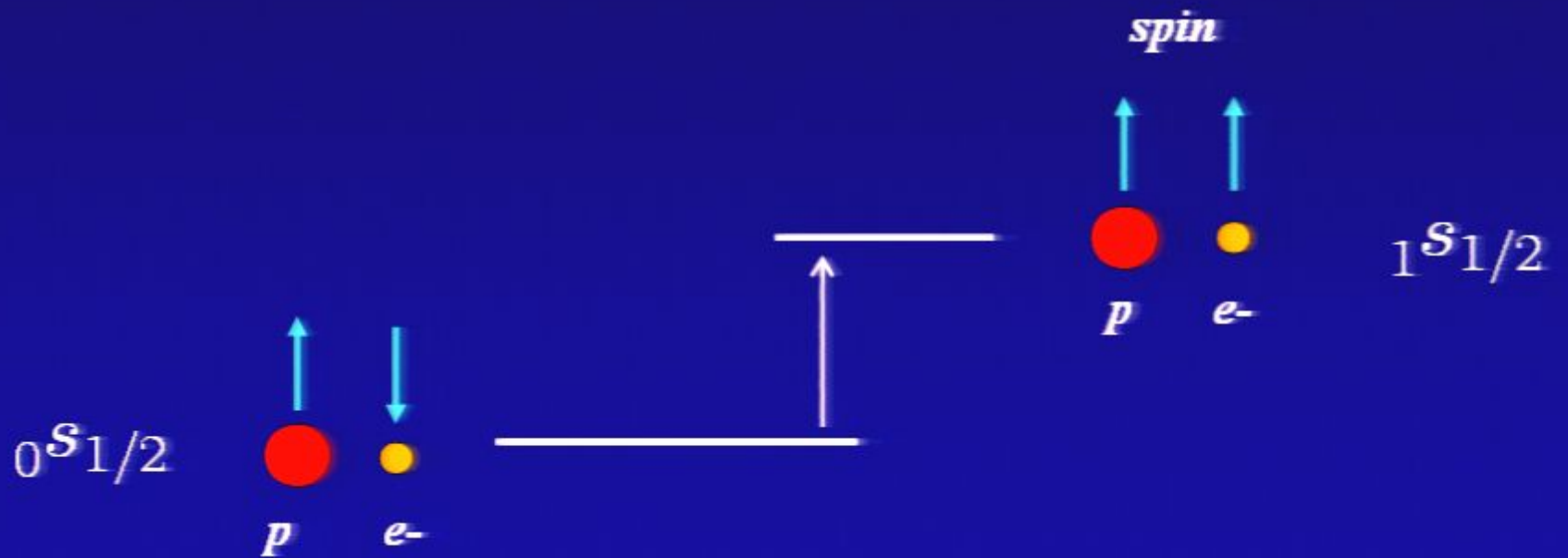
Launch date: 2013

Extremely Large Telescopes (20-40 meters)



- GMT=Seven mirrors, each 8.4m in diameter
- TMT, EELT – segmented 20-40m aperture

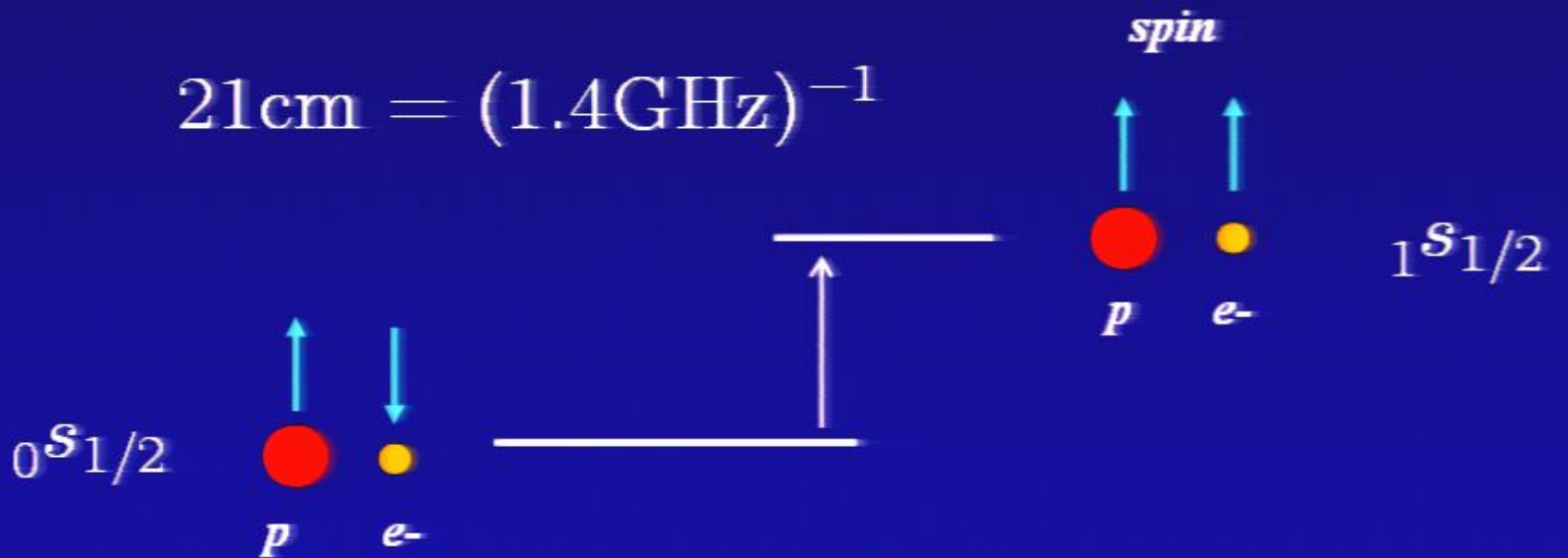
Mapping the Cosmic Distribution of Hydrogen



Mapping the Cosmic Distribution of Hydrogen



$$21\text{cm} = (1.4\text{GHz})^{-1}$$

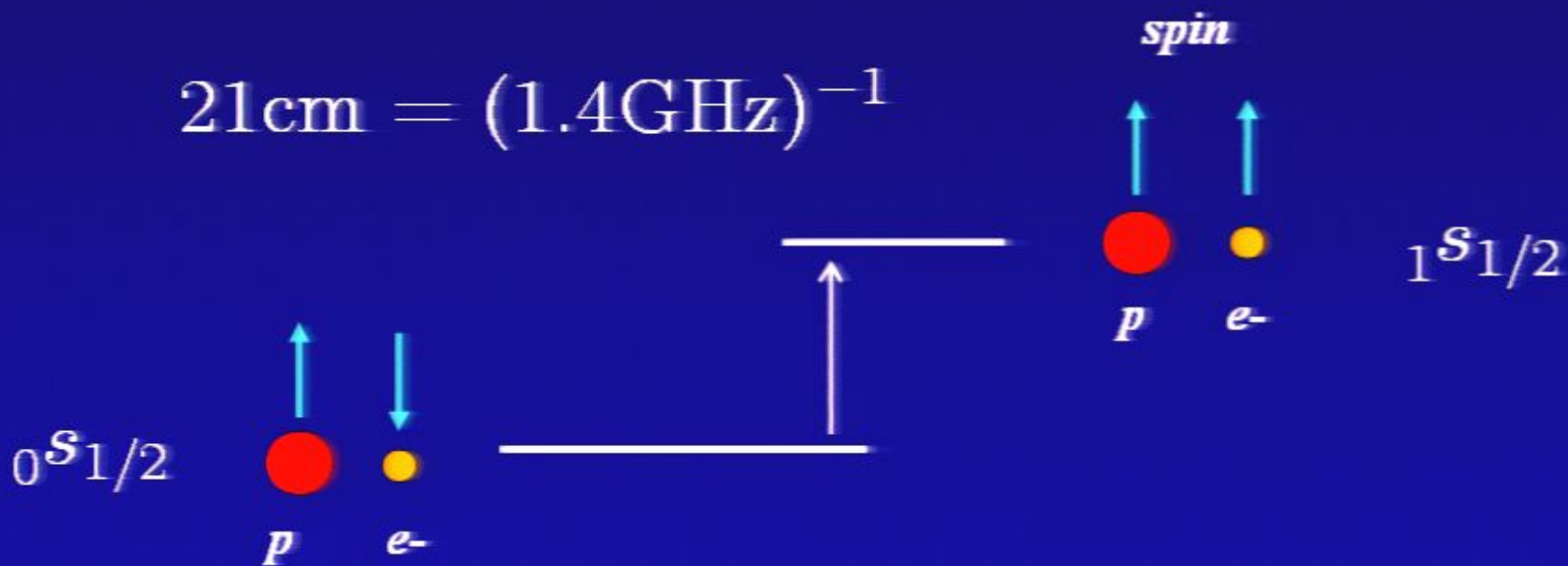


Mapping the Cosmic Distribution of Hydrogen



excitation rate = (atomic collisions) + (radiative coupling to CMB)

$$21\text{cm} = (1.4\text{GHz})^{-1}$$



Spin Temperature

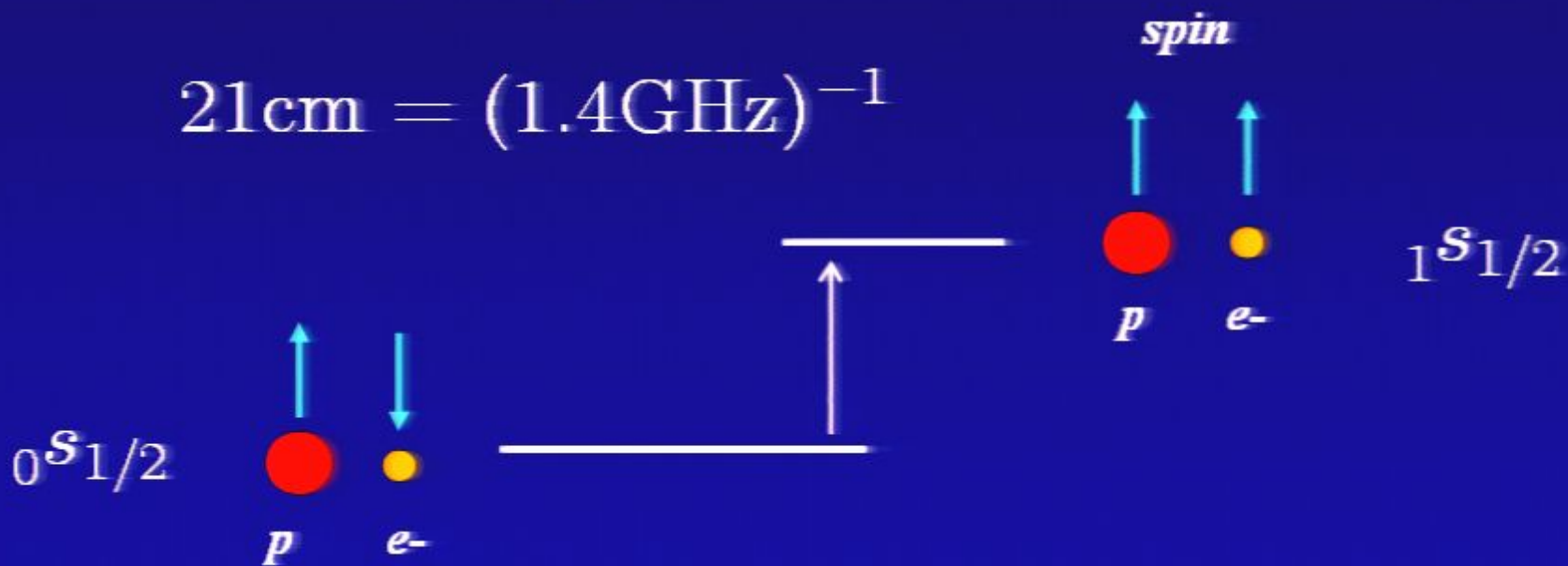
$$\frac{n_1}{n_0} = \frac{g_1}{g_0} \exp\left\{-\frac{0.068\text{K}}{T_s}\right\} \quad (g_1/g_0) = 3$$

Mapping the Cosmic Distribution of Hydrogen



excitation rate = (atomic collisions) + (radiative coupling to CMB)
 Couple T_s to

$$21\text{cm} = (1.4\text{GHz})^{-1}$$



Spin Temperature

$$\frac{n_1}{n_0} = \frac{g_1}{g_0} \exp\left\{-\frac{0.068\text{K}}{T_s}\right\} \quad (g_1/g_0) = 3$$

Mapping the Cosmic Distribution of Hydrogen



excitation rate = (atomic collisions) + (radiative coupling to CMB)

Couple T_s to T_k

Couples to

spin

$$21\text{cm} = (1.4\text{GHz})^{-1}$$



Spin Temperature

$$\frac{n_1}{n_0} = \frac{g_1}{g_0} \exp\left\{-\frac{0.068\text{K}}{T_s}\right\}$$

$$(g_1/g_0) = 3$$

Mapping the Cosmic Distribution of Hydrogen



excitation rate = (atomic collisions) + (radiative coupling to CMB)

Couple T_s to T_k Couples T_s to T_γ

$$21\text{cm} = (1.4\text{GHz})^{-1}$$



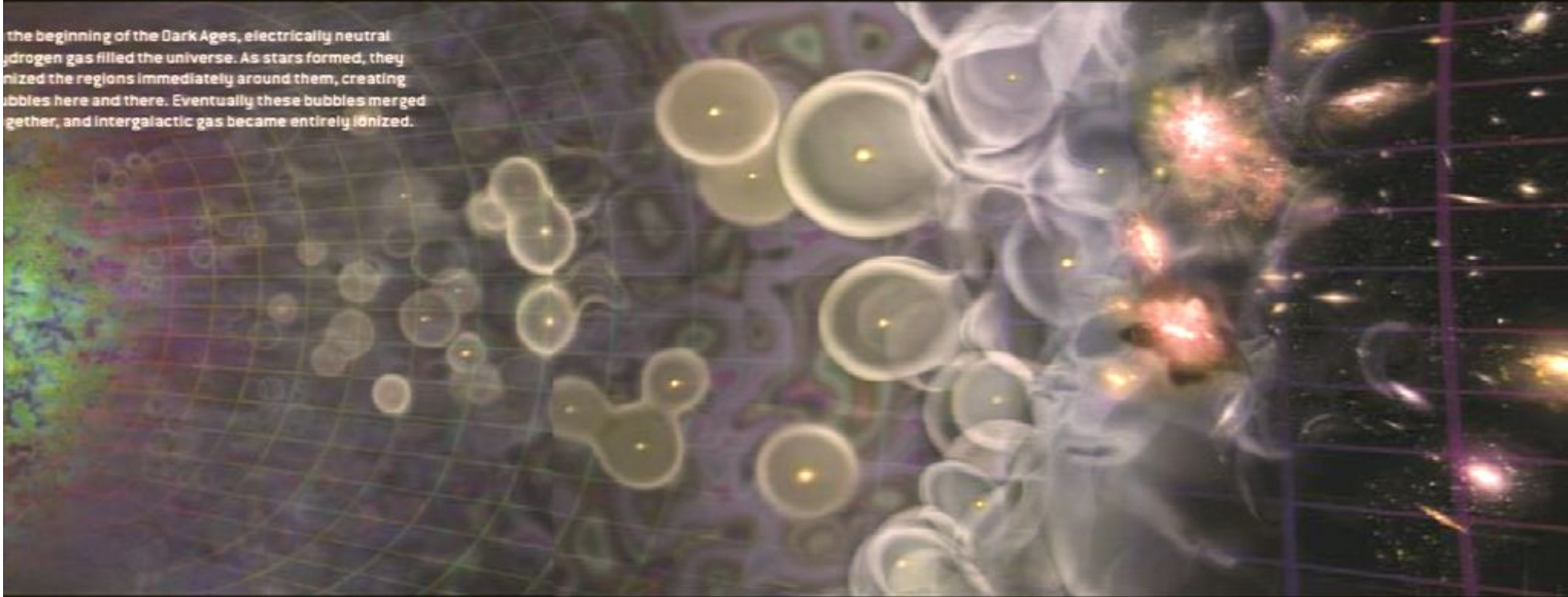
Spin Temperature

$$\frac{n_1}{n_0} = \frac{g_1}{g_0} \exp\left\{-\frac{0.068\text{K}}{T_s}\right\} \quad (g_1/g_0) = 3$$

21cm Mapping of Cosmic History

BRIGHTENING UP THE COSMOS

At the beginning of the Dark Ages, electrically neutral hydrogen gas filled the universe. As stars formed, they ionized the regions immediately around them, creating bubbles here and there. Eventually these bubbles merged together, and intergalactic gas became entirely ionized.



Time:
Width of frame:
Observed wavelength:

210 million years:
2.4 million light-years:
4.1 meters:

All the gas is neutral. The white areas are the densest and will give rise to the first stars and quasars.

290 million years:
3.0 million light-years:
3.3 meters:

Faint red patches show that the stars and quasars have begun to ionize the gas around them.

370 million years:
3.6 million light-years:
2.8 meters:

These bubbles of ionized gas grow.

460 million years:
4.1 million light-years:
2.4 meters:

New stars and quasars form and create their own bubbles.

540 million years:
4.6 million light-years:
2.1 meters:

The bubbles are beginning to interconnect.

620 million years:
5.0 million light-years:
2.0 meters:

The bubbles have merged and nearly taken over all of space.

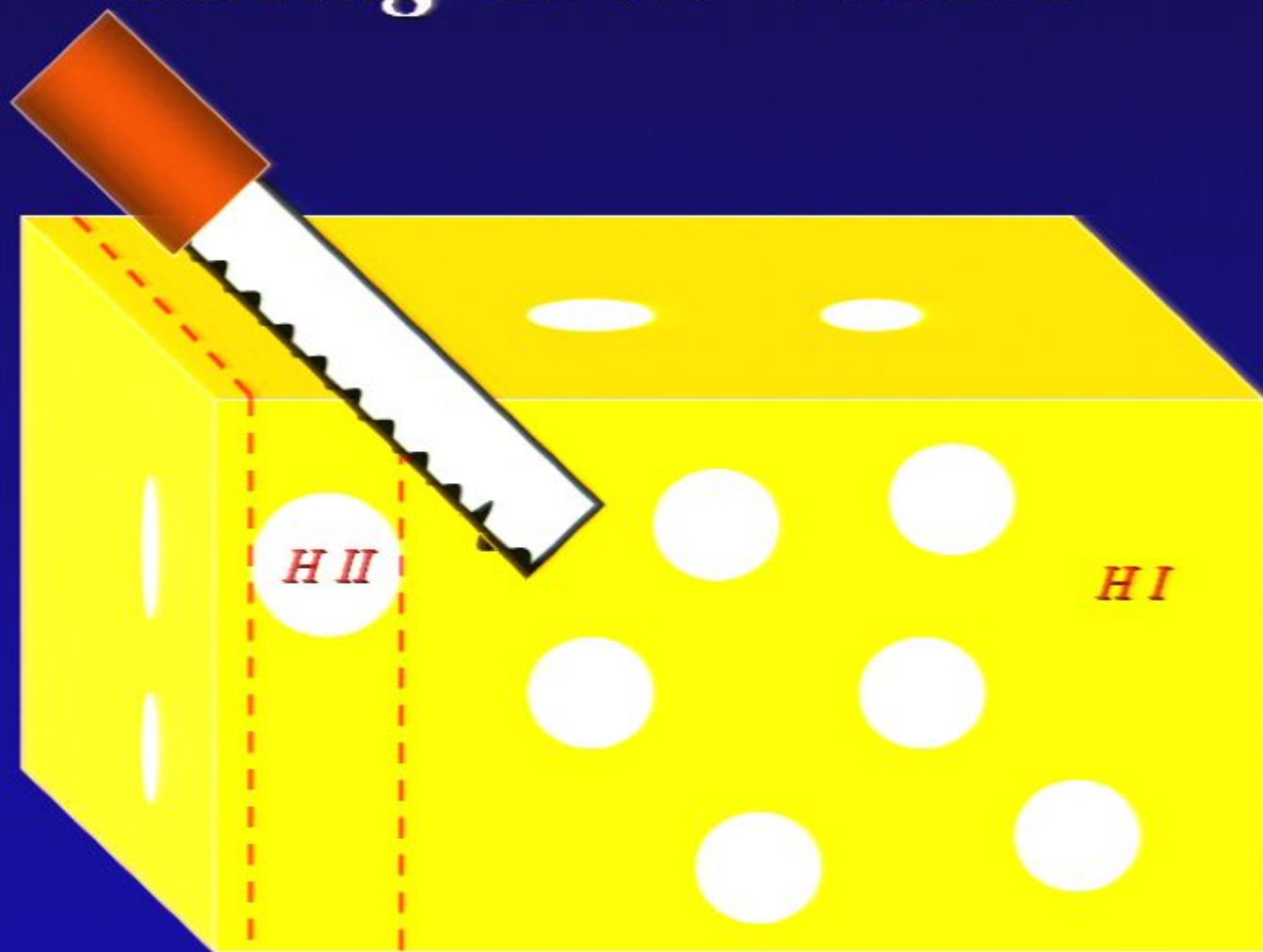
710 million years:
5.5 million light-years:
1.8 meters:

The only neutral hydrogen is concentrated in galaxies.

Simulated images of 21-centimeter radiation show how hydrogen gas turns into a galaxy cluster. The amount of radiation (white is highest; orange and red are intermediate; black is least) reflects both the density of the gas and its degree of ionization: dense, electrically neutral gas appears white; dense, ionized gas appears black. The images have been rescaled to remove the effect of cosmic expansion and thus highlight the cluster-forming processes. Because of expansion, the 21-centimeter radiation is actually observed at a longer wavelength; the earlier the image, the longer the wavelength.



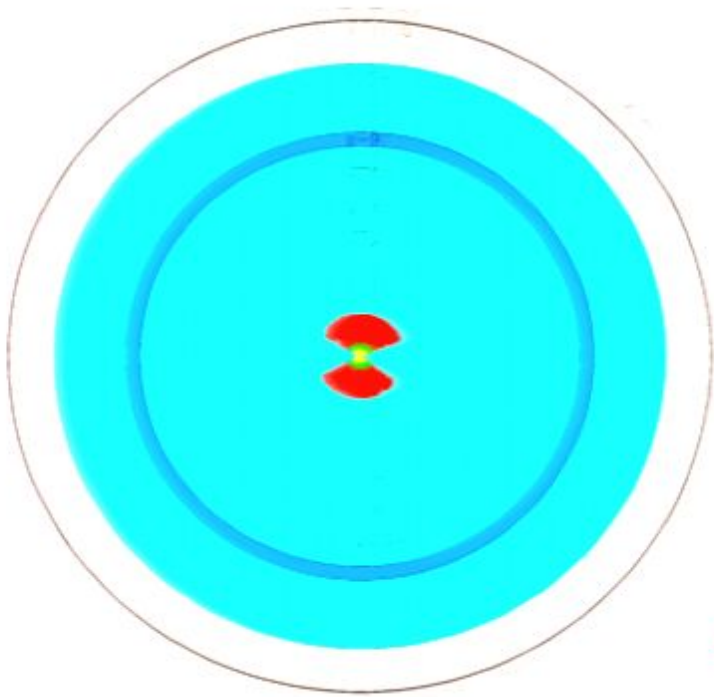
*21cm Tomography of Ionized Bubbles During Reionization is like
Slicing Swiss Cheese*



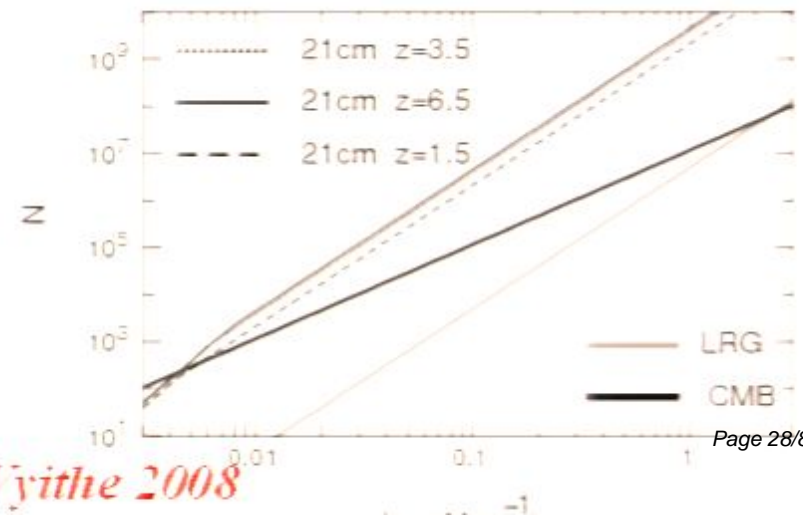
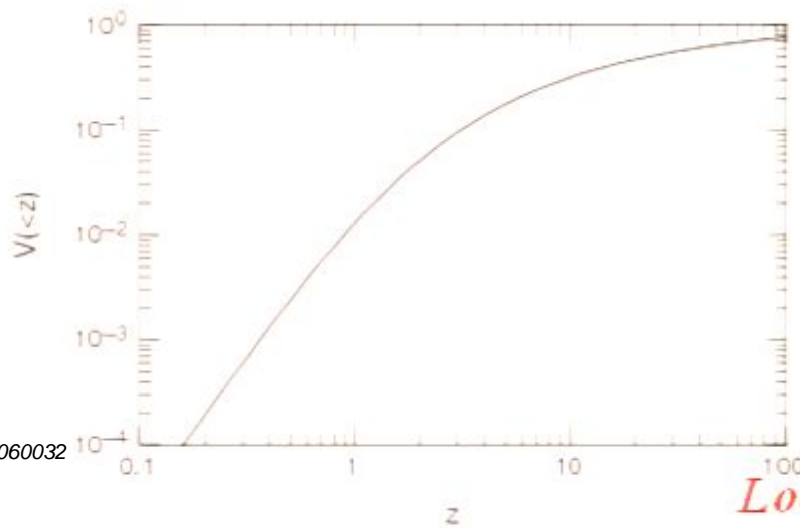
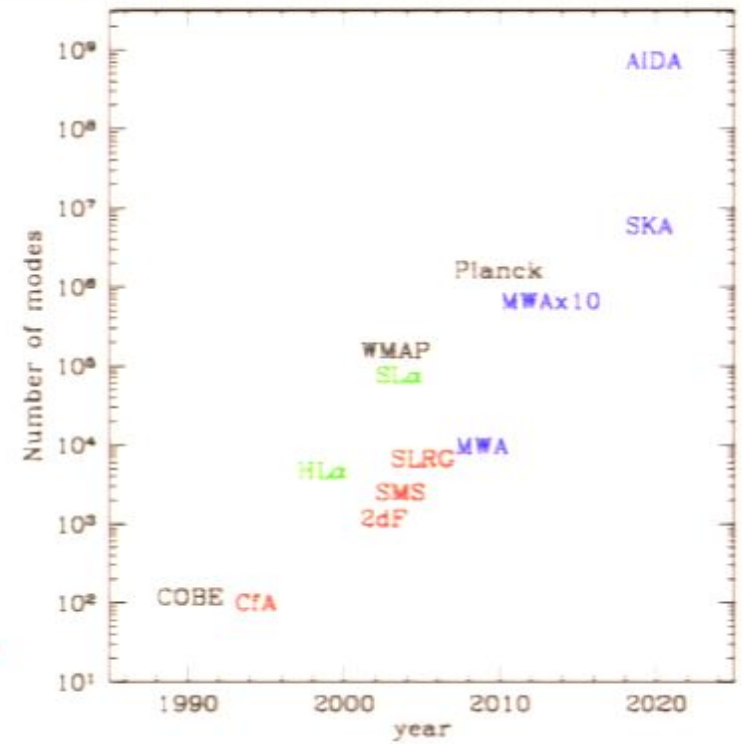
Observed wavelength \leftrightarrow distance

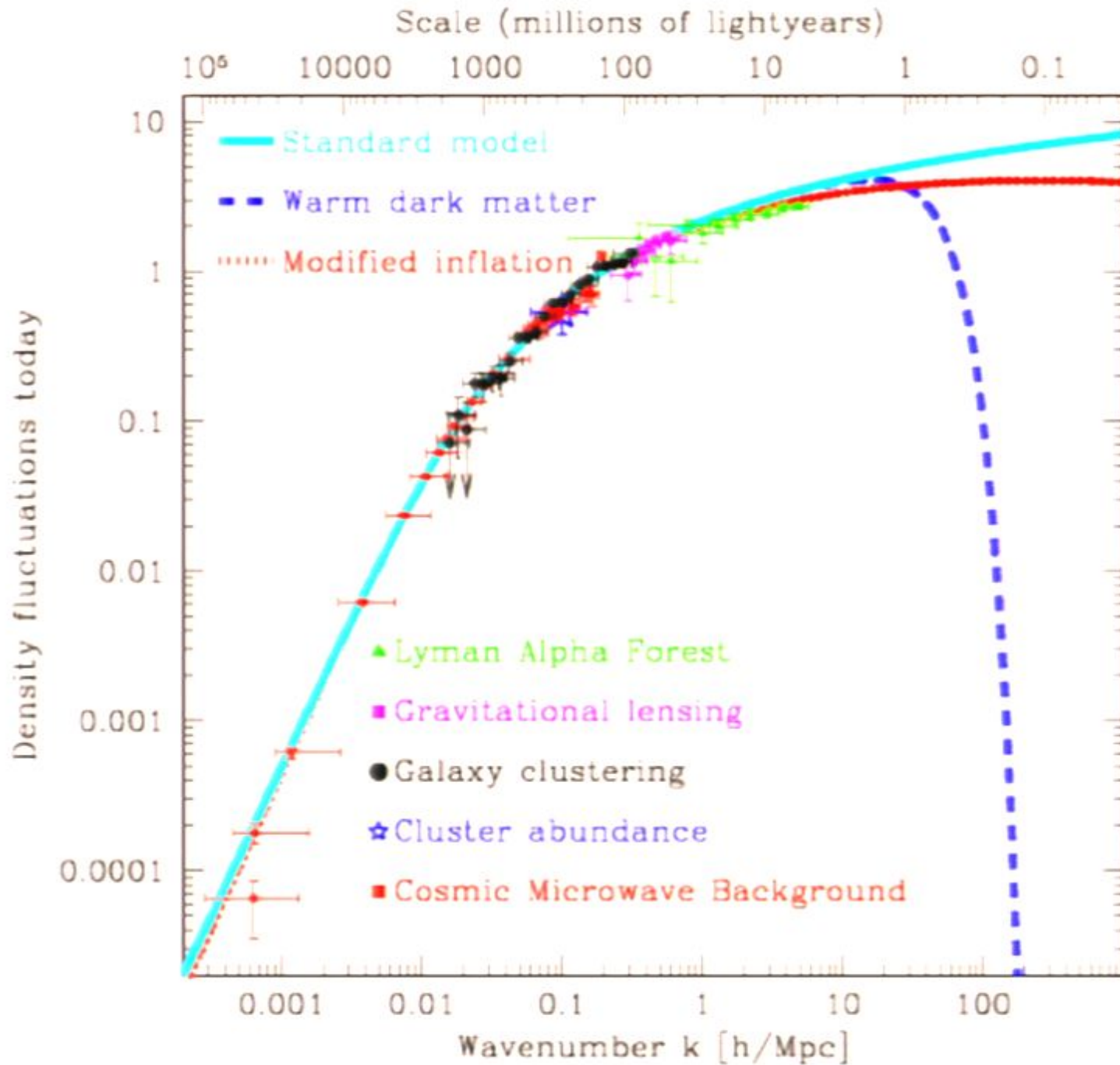
$$21\text{cm} \times (1 + z)$$

Counting Modes in Cosmological Surveys



Mao et al. 2008





Separating the Physics from the Astrophysics

Separating the Physics from the Astrophysics

Physics: initial conditions from inflation;
nature of dark matter and dark energy

Astrophysics: consequences of star formation

Separating the Physics from the Astrophysics

Physics: initial conditions from inflation;
nature of dark matter and dark energy

Astrophysics: consequences of star formation

Three epochs:

Separating the Physics from the Astrophysics

Physics: initial conditions from inflation;
nature of dark matter and dark energy

Astrophysics: consequences of star formation

Three epochs:

- Before the first galaxies ($z > 25$): mapping of density fluctuations through 21cm absorption

Separating the Physics from the Astrophysics

Physics: initial conditions from inflation;
nature of dark matter and dark energy

Astrophysics: consequences of star formation

Three epochs:

- Before the first galaxies ($z > 25$): mapping of density fluctuations through 21cm absorption
- During reionization: anisotropy of the 21cm power spectrum due to peculiar velocities

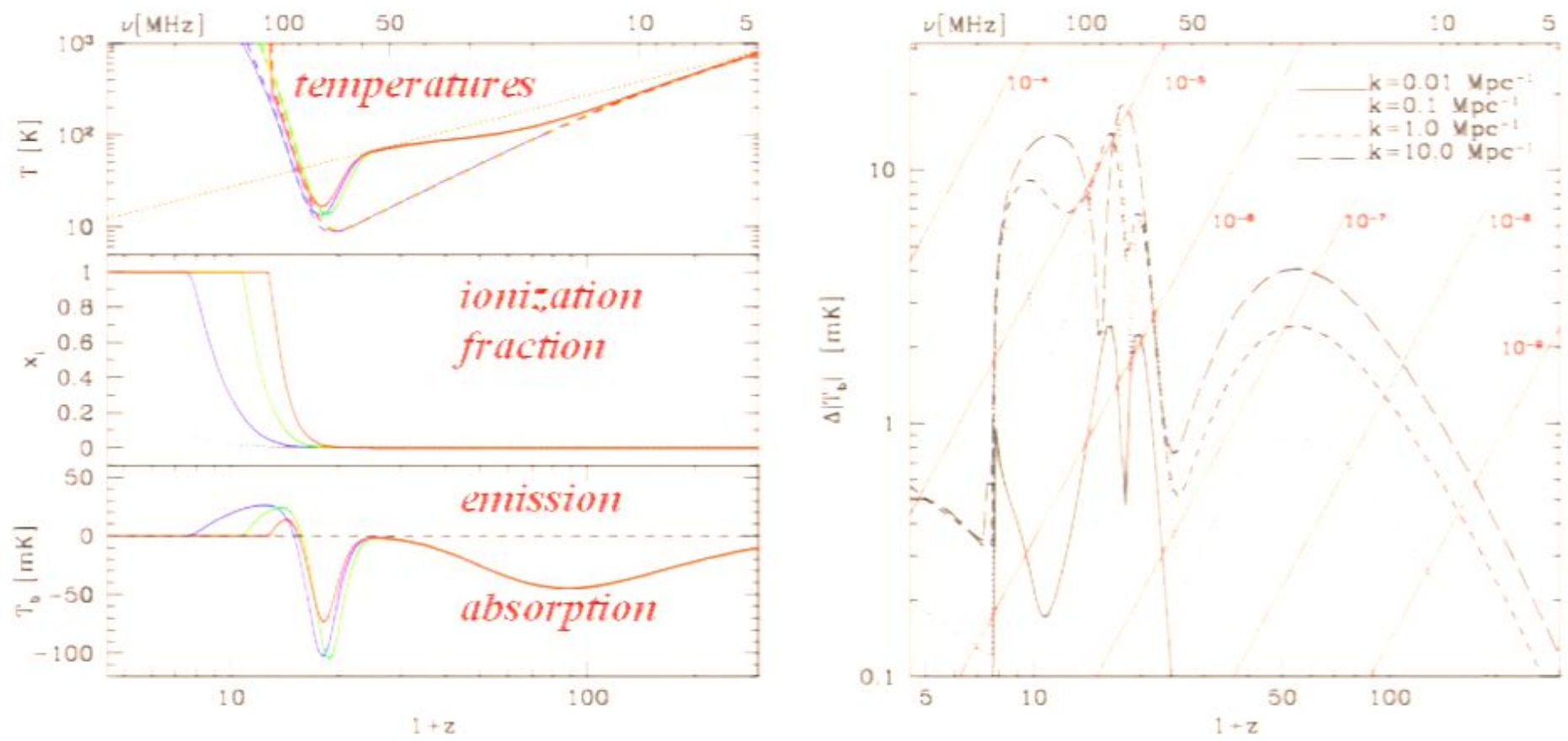
Separating the Physics from the Astrophysics

Physics: initial conditions from inflation;
nature of dark matter and dark energy

Astrophysics: consequences of star formation

Three epochs:

- **Before the first galaxies ($z > 25$):** mapping of density fluctuations through 21cm absorption
- **During reionization:** anisotropy of the 21cm power spectrum due to peculiar velocities
- **After reionization ($z < 6$):** dense pockets of residual hydrogen (DLAs) trace large scale structure

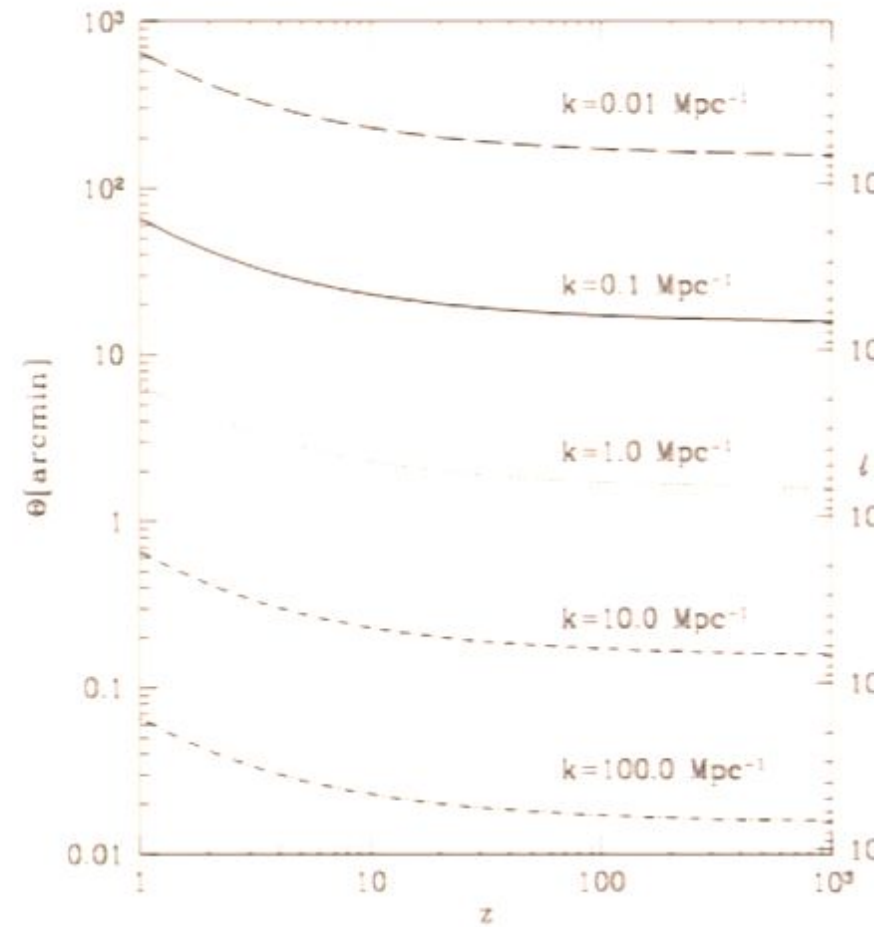
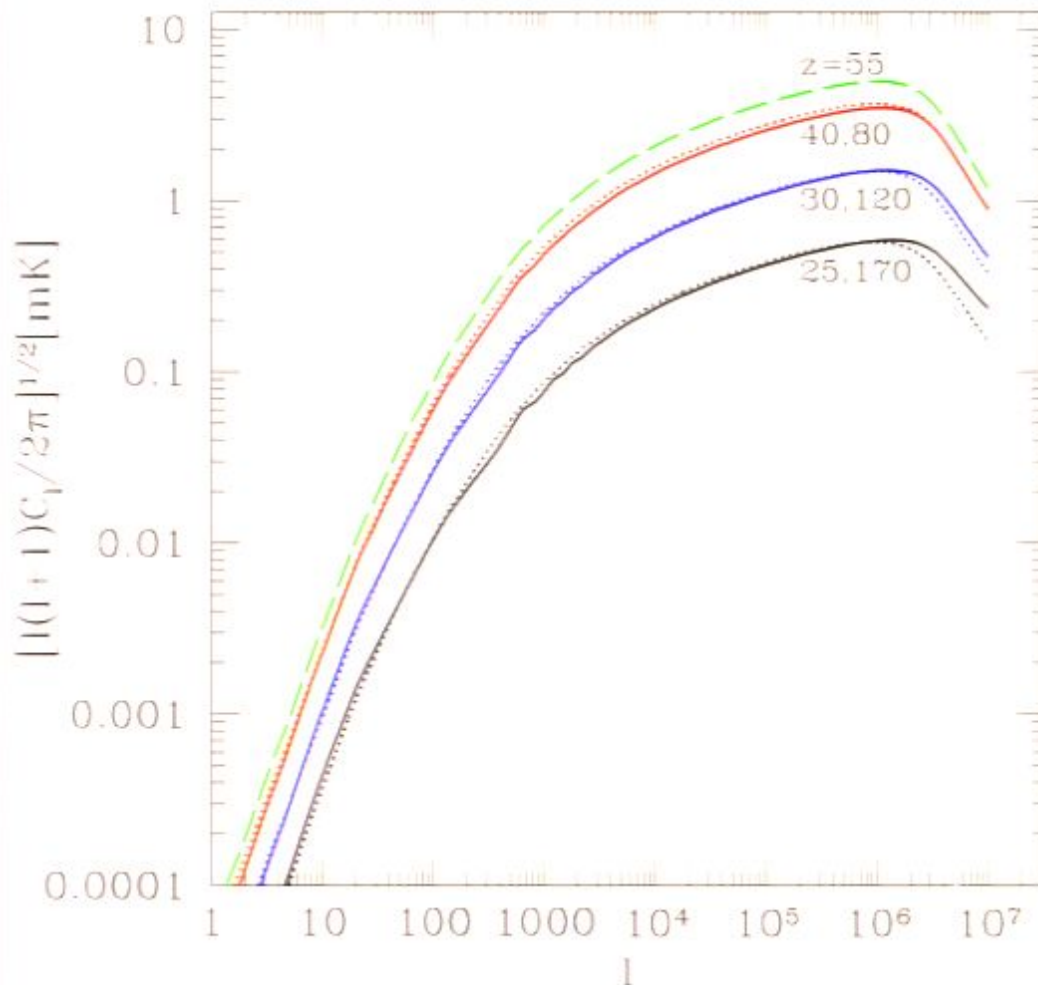


Left: Top panel: Evolution of the mean CMB (dotted curve), intergalactic medium (IGM, dashed curve), and spin (solid curve) temperatures. Middle panel: Evolution of the filling fraction of ionized bubbles (solid curve) and electron fraction outside the bubbles (dotted curve). Bottom panel: Evolution of mean 21cm brightness temperature. Three different astrophysical models are plotted, corresponding to the -1σ (red curve), best-fit (green curve), and $+1\sigma$ (blue curve) optical depth values derived from WMAP [1]. Right: Redshift evolution of the angle-averaged 21cm power spectrum $\bar{\Delta T}_b$ in the -1σ model for wave-numbers $k = 0.01$ (solid curve), 0.1 (dotted curve), 1.0 (short dashed curve), and 10.0 Mpc $^{-1}$ (long dashed curve). Diagonal lines indicate the foreground brightness of the sky $T_{\text{sky}}(\nu)$ times a factor r ranging from 10^{-4} to 10^{-9} , indicative of the level of foreground subtraction required (Deichard & Luuk 2009).

21 cm Absorption During the Dark Ages

$$T_b = \tau \left(\frac{T_s - T_\gamma}{1+z} \right)$$

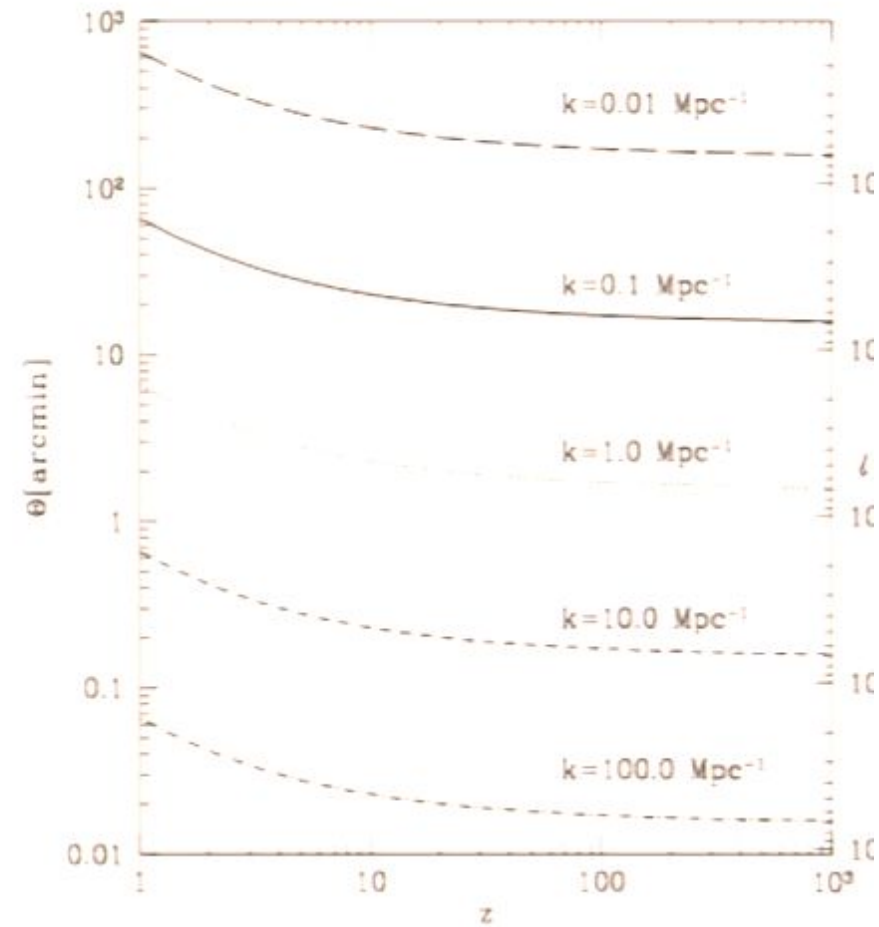
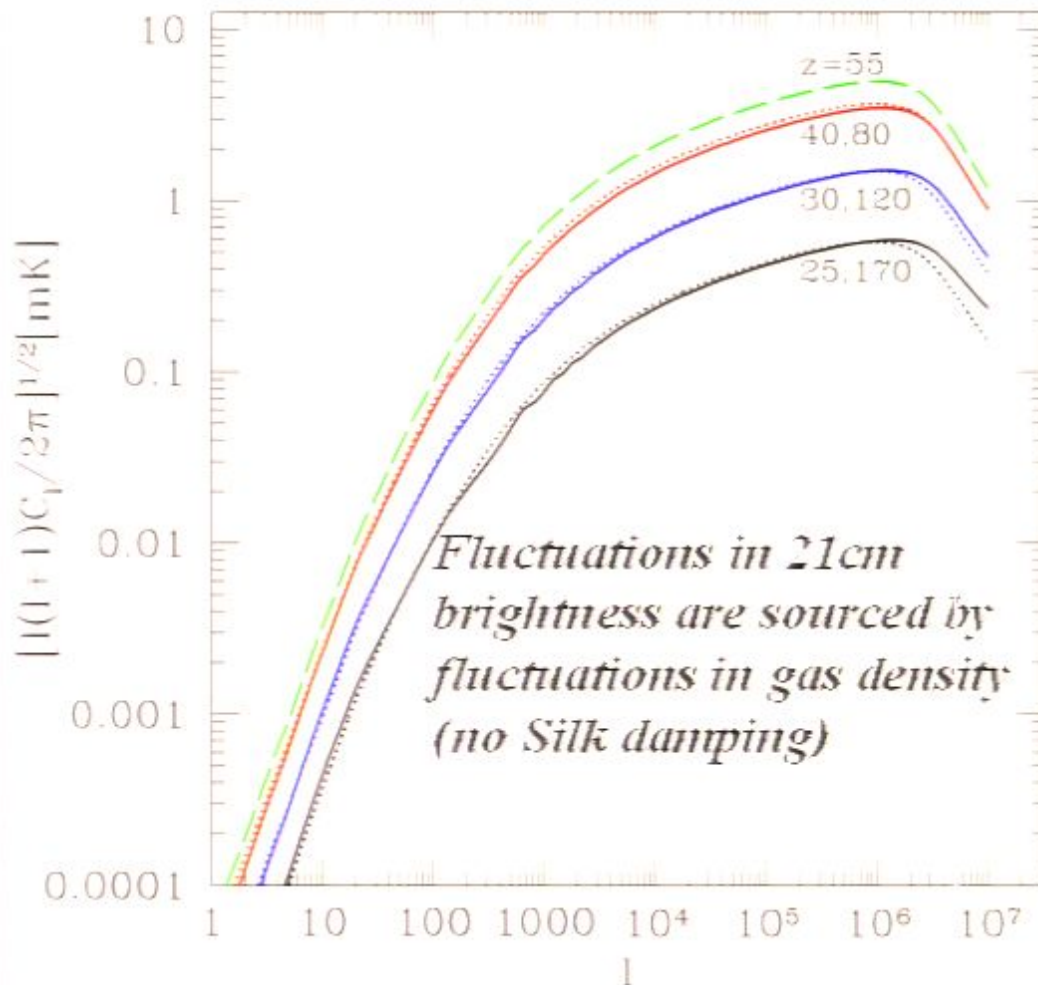
$$T_b = 28\text{mK} \left(\frac{1+z}{10} \right)^{1/2} \left(\frac{T_s - T_\gamma}{T_s} \right)$$



21 cm Absorption During the Dark Ages

$$T_b = \tau \left(\frac{T_s - T_\gamma}{1+z} \right)$$

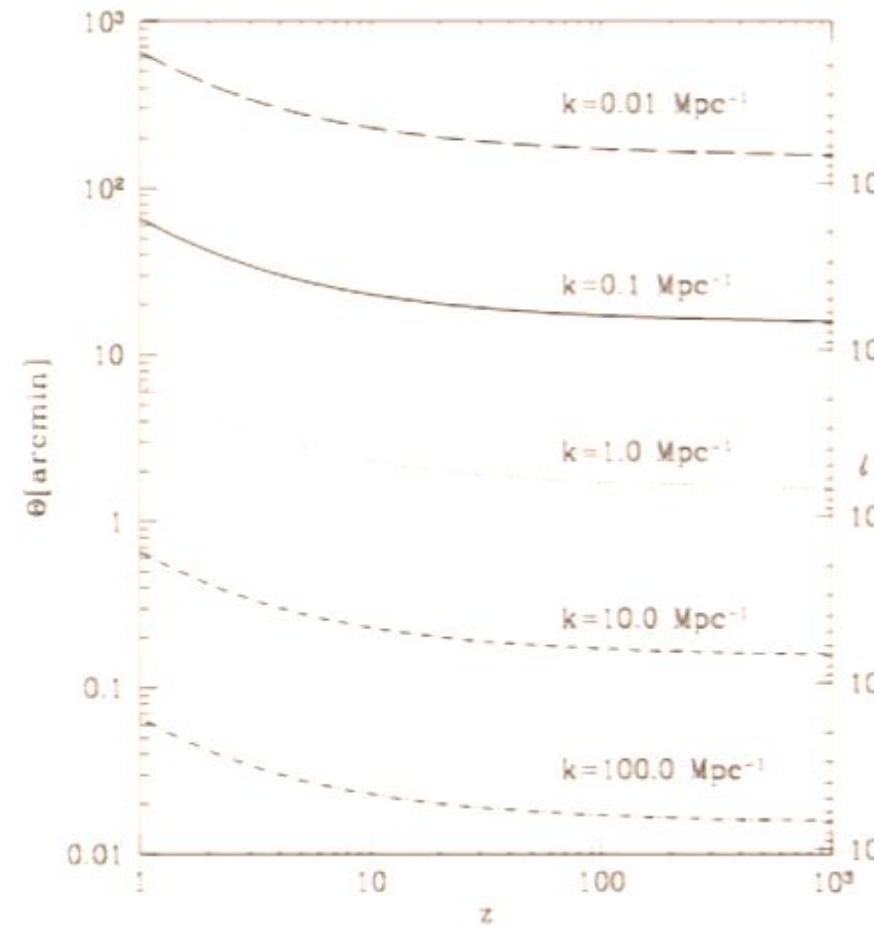
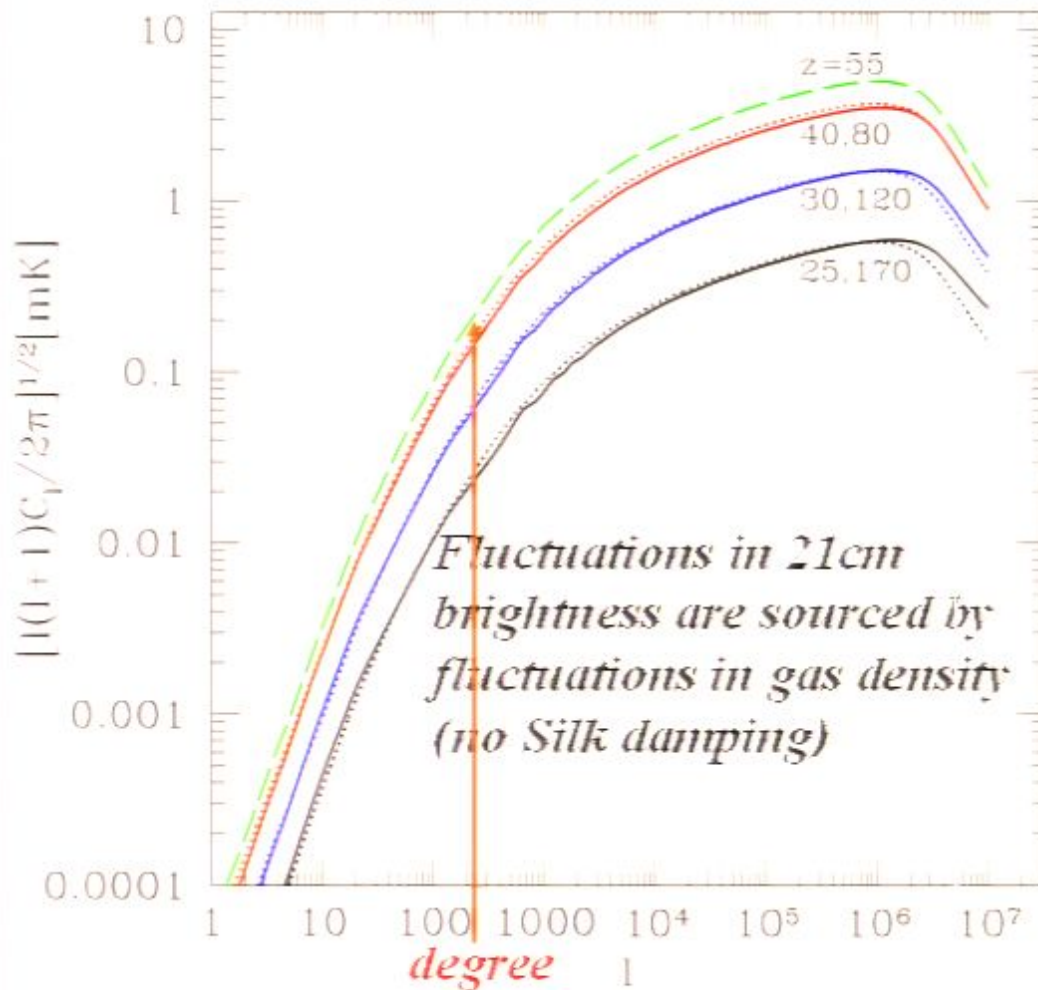
$$T_b = 28\text{mK} \left(\frac{1+z}{10} \right)^{1/2} \left(\frac{T_s - T_\gamma}{T_s} \right)$$



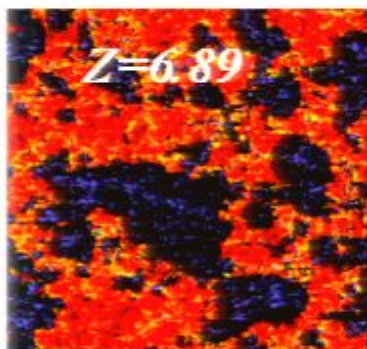
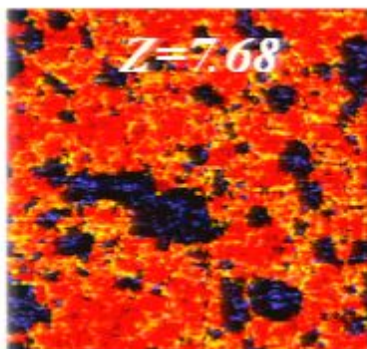
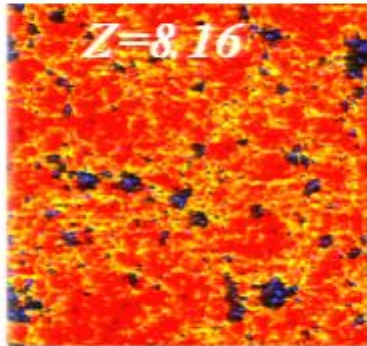
21 cm Absorption During the Dark Ages

$$T_b = \tau \left(\frac{T_s - T_\gamma}{1+z} \right)$$

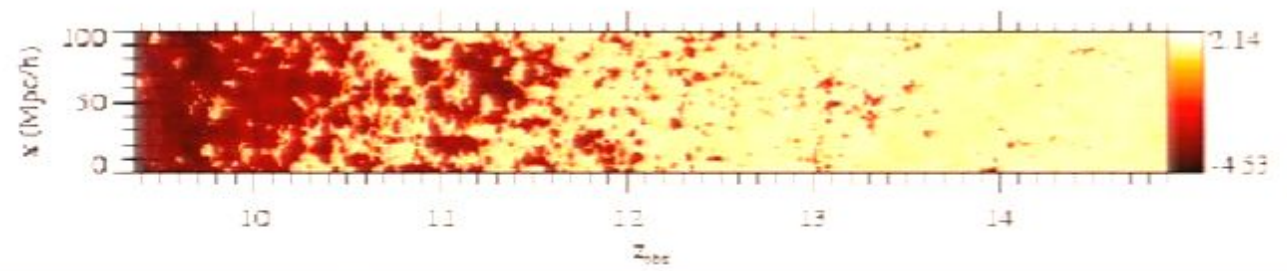
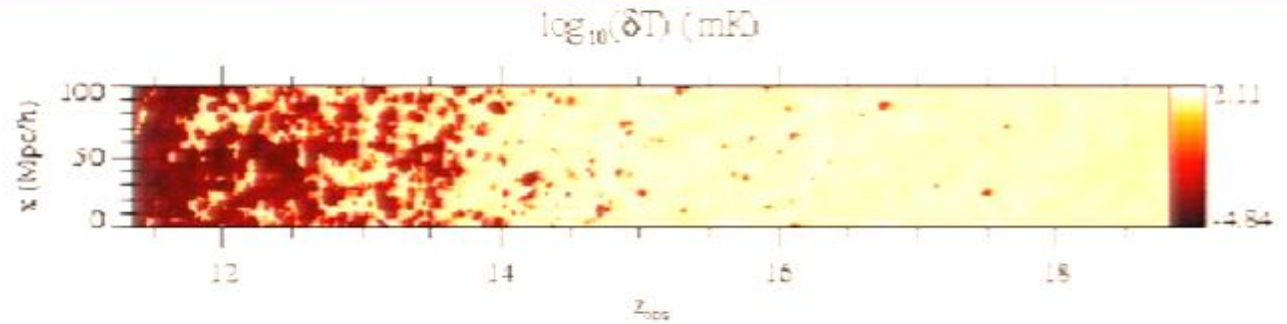
$$T_b = 28\text{mK} \left(\frac{1+z}{10} \right)^{1/2} \left(\frac{T_s - T_\gamma}{T_s} \right)$$



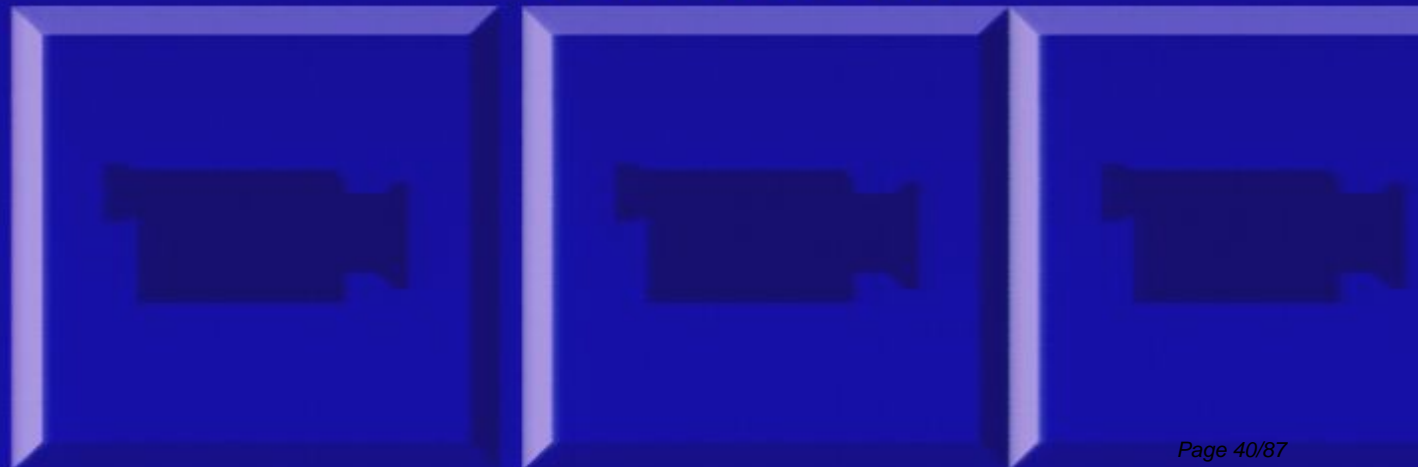
HI Density



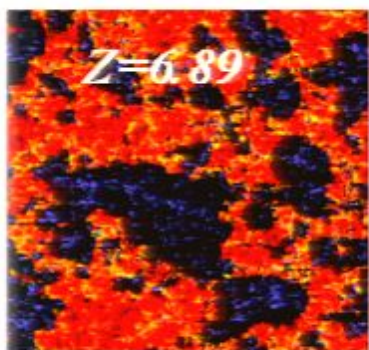
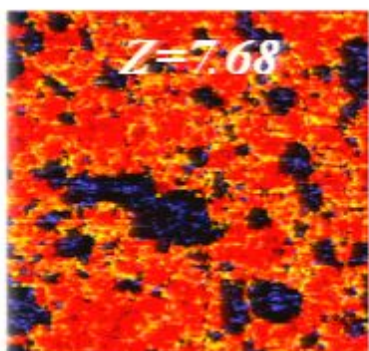
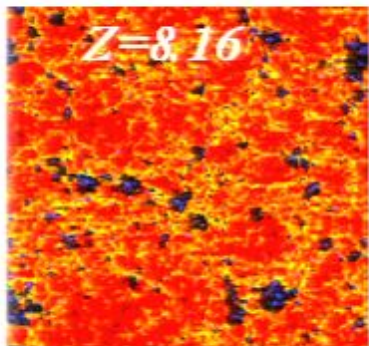
21cm Mapping of Epoch of Reionization



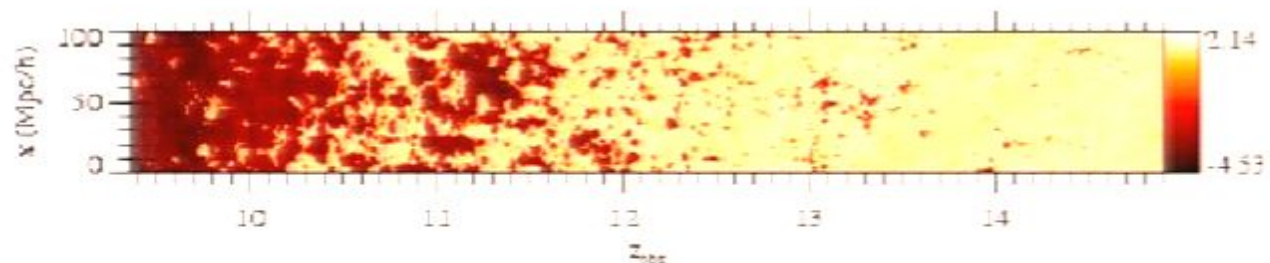
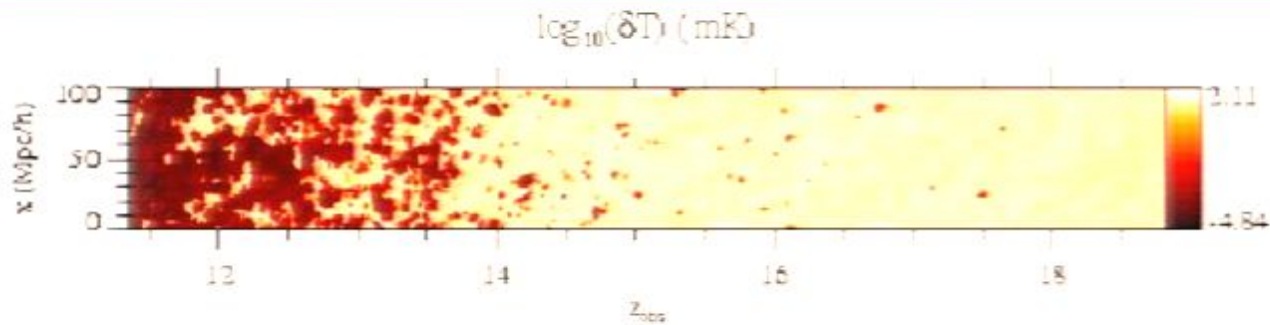
Mellema et al 2006



HI Density



21cm Mapping of Epoch of Reionization



Mellema et al 2006



Windows Media Player

Now Playing Library Rip Burn Sync Guide

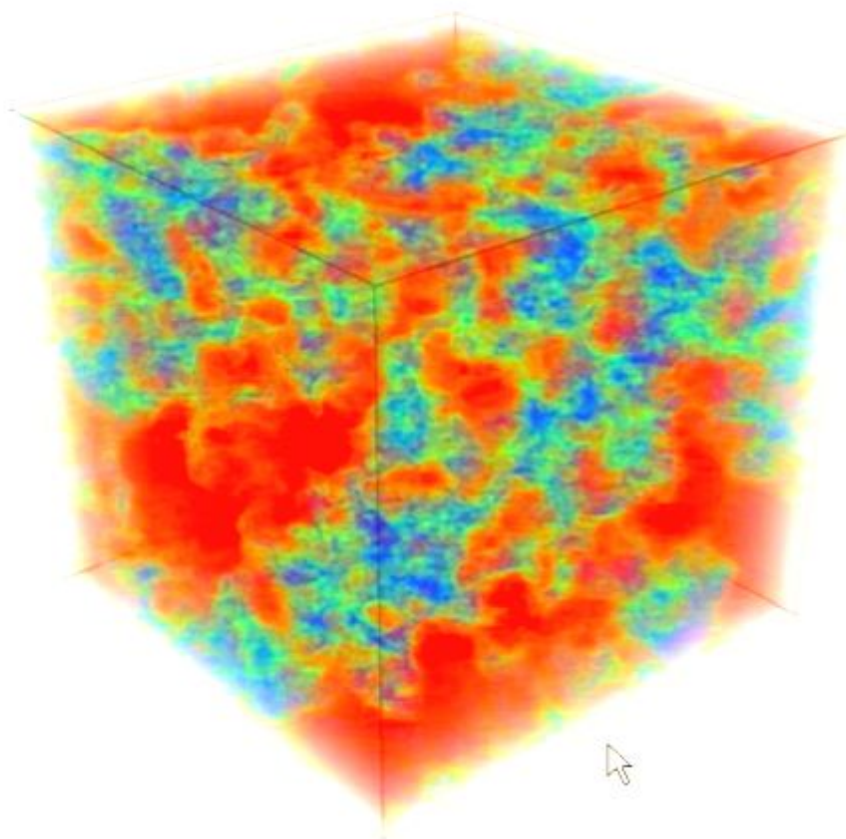


Windows Media Player

Now Playing Library Rip Burn Sync Guide

Now Playing List

$z = 08.0831$



Shin et al. 2007

HI 0:

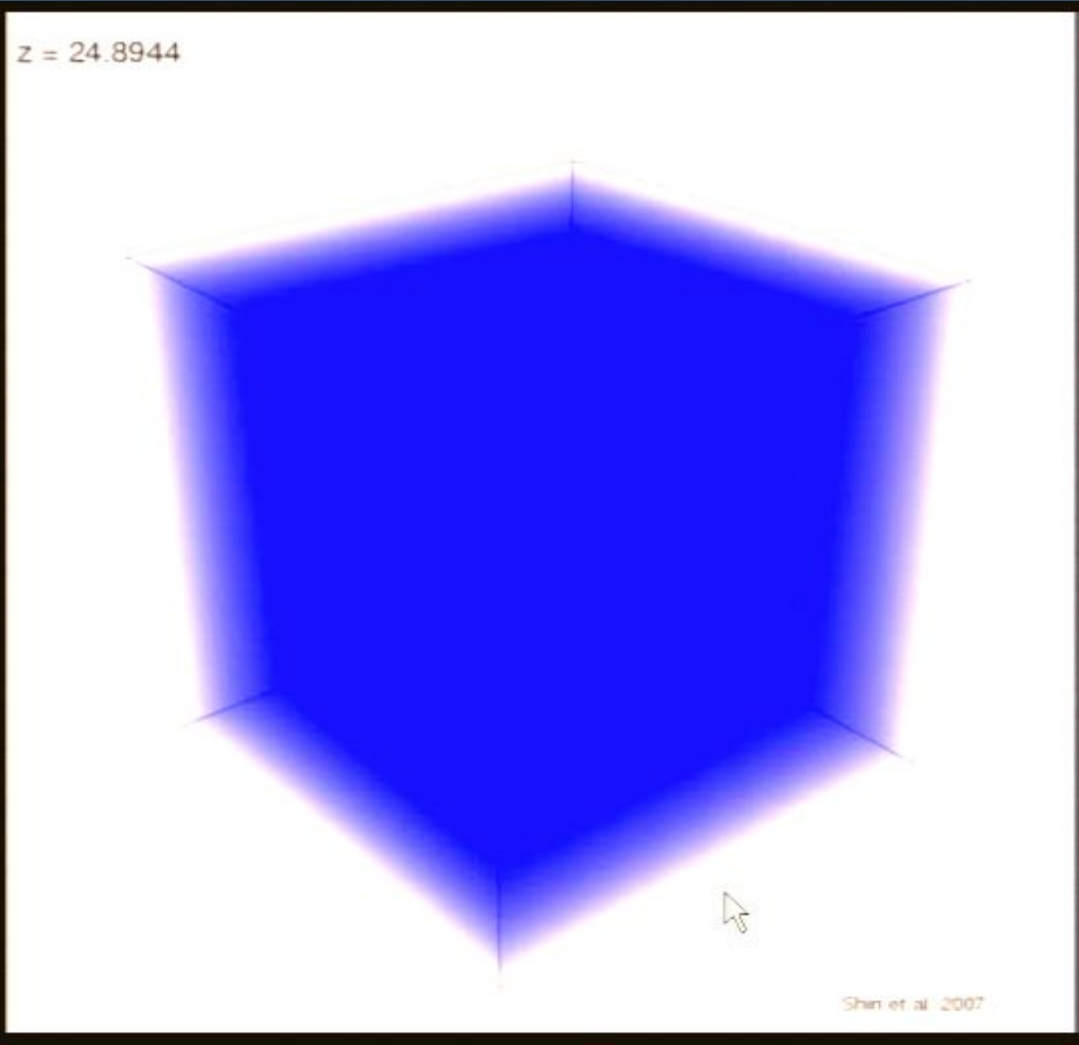


HI

Windows Media Player

Now Playing Library Rip Burn Sync Guide

Now Playing List



HI 0:

Total Time: 0

HI

Pirsa: 08060032

Stopped

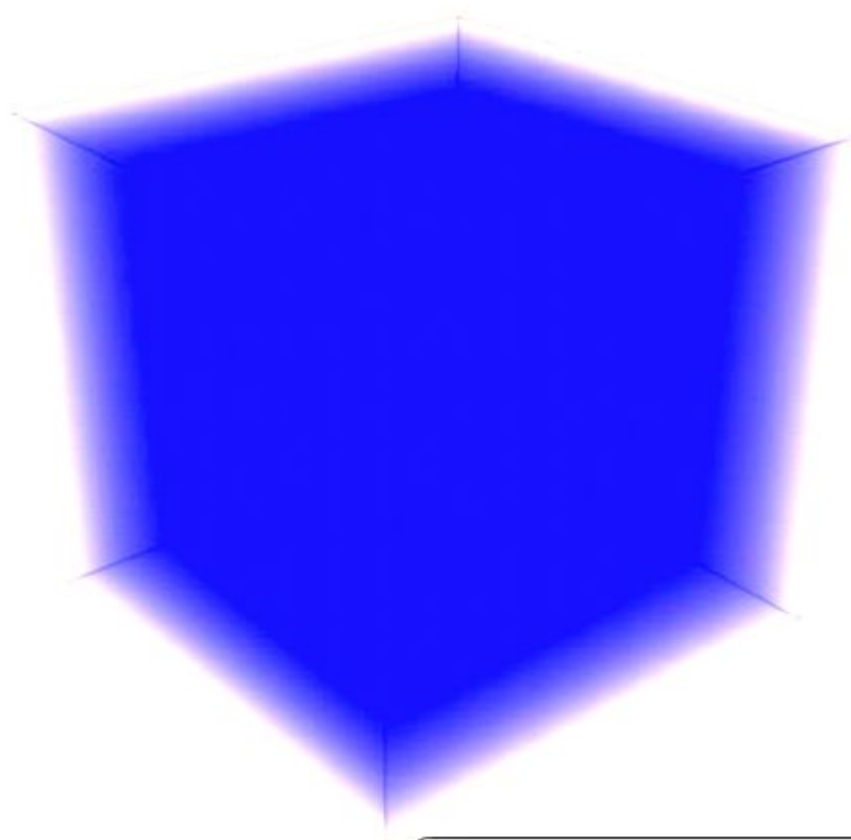
Page 44/87

Windows Media Player

Now Playing Library Rip Burn Sync Guide

Now Playing List

$z = 24.8944$



HI 0:

Total Time: 0



Wireless networks detected

One or more wireless networks are in range of this computer. To see the list and connect, click this message

HI Density

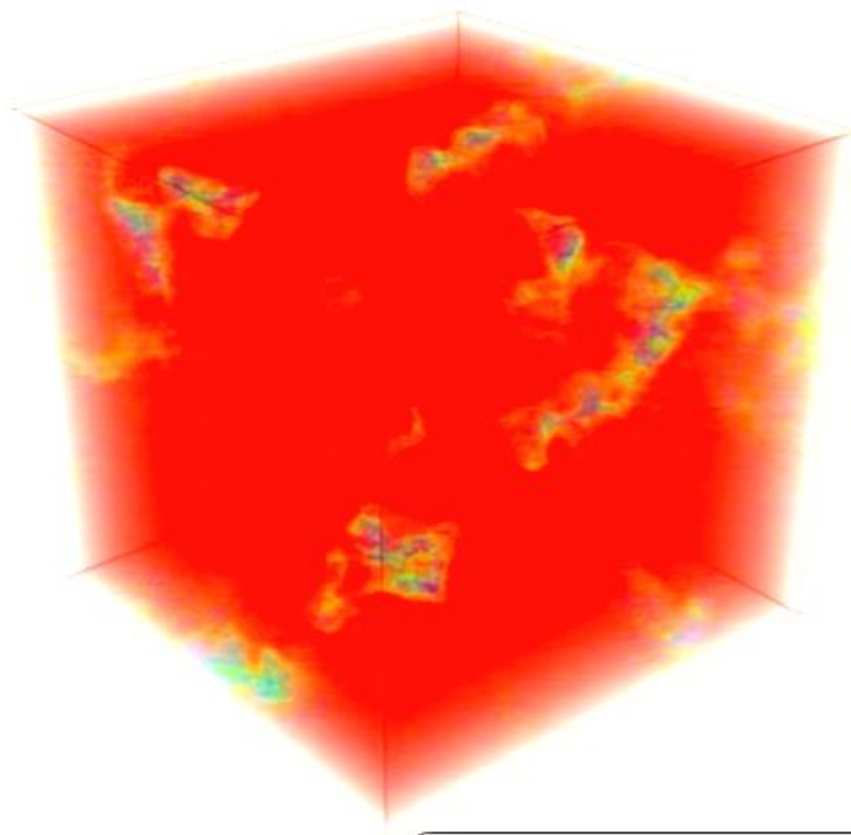
21cm Mapping of Epoch of Reionization

Windows Media Player

Now Playing Library Rip Burn Sync Guide

Now Playing List

$z = 06.4610$



HI 0:

Total Time: 0



Wireless networks detected X

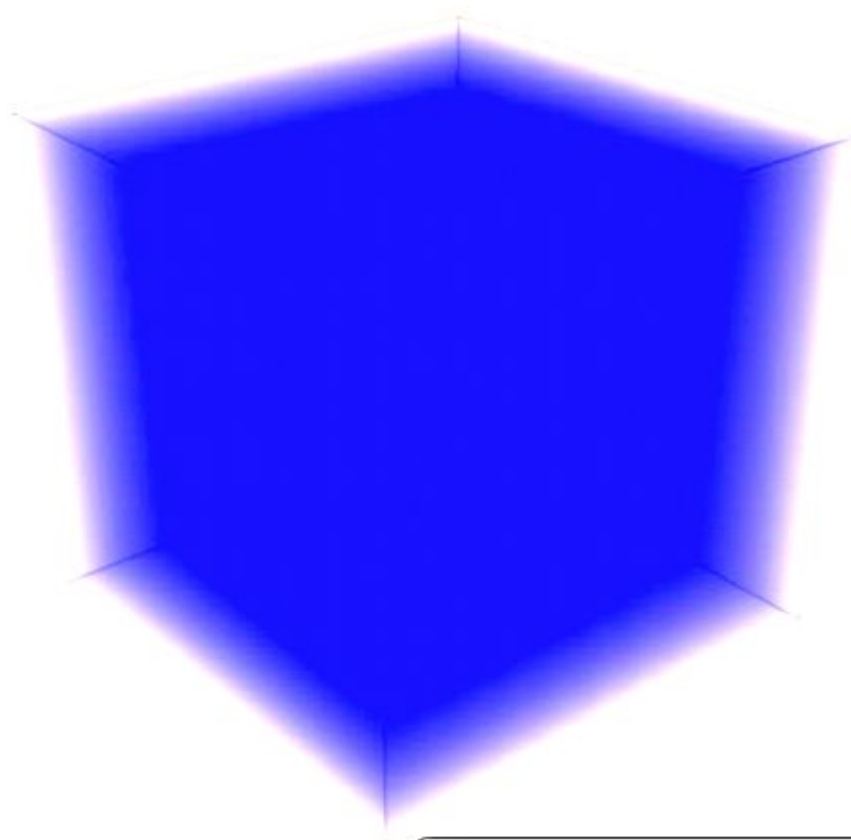
One or more wireless networks are in range of this computer. To see the list and connect, click this message

Windows Media Player

Now Playing Library Rip Burn Sync Guide

Now Playing List

$z = 24.8944$



HI 0:

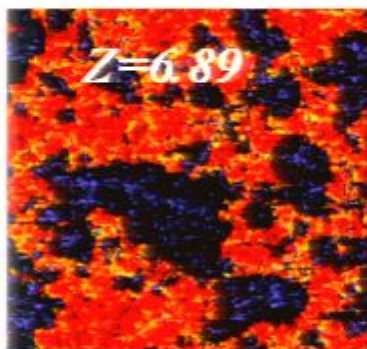
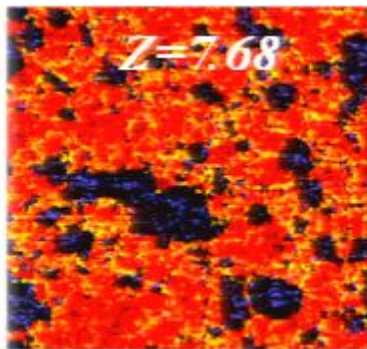
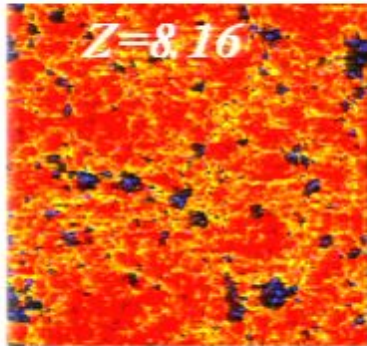
Total Time: 0



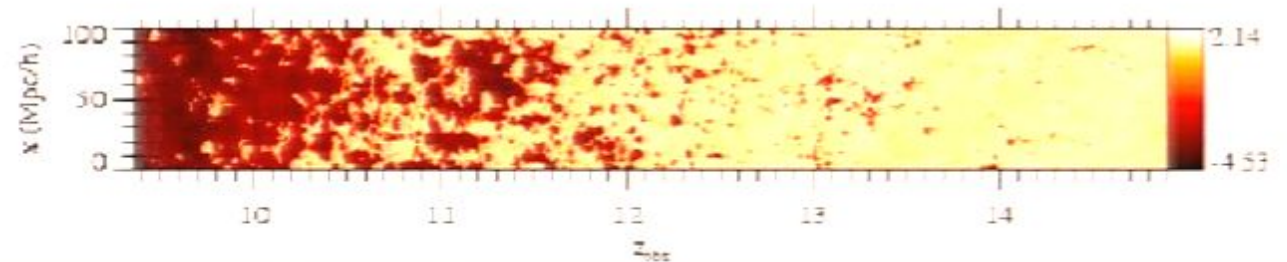
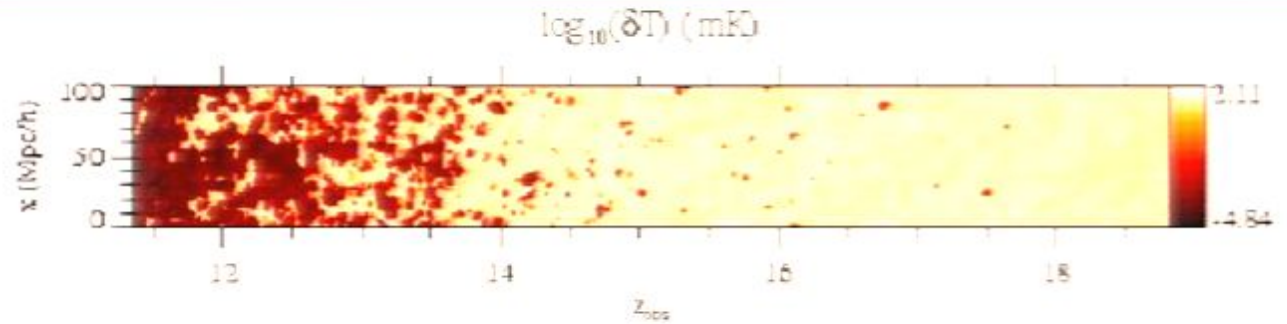
Wireless networks detected

One or more wireless networks are in range of this computer. To see the list and connect, click this message

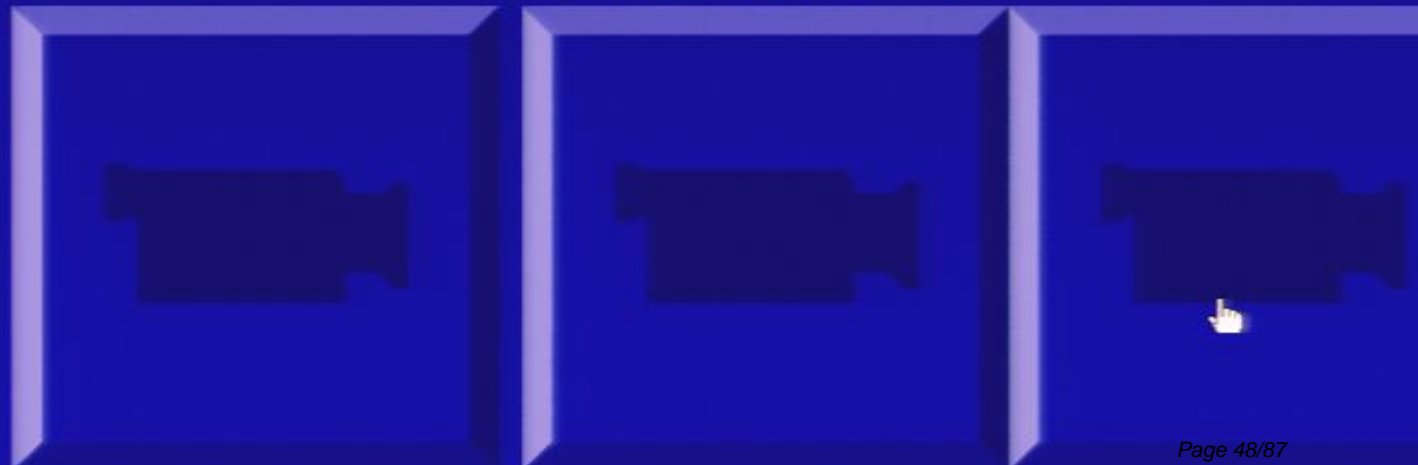
HI Density



21cm Mapping of Epoch of Reionization



Mellema et al 2006



Line-of-Sight Anisotropy of 21cm Flux Fluctuations

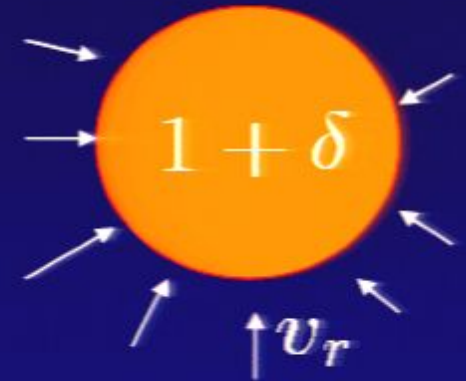
$$T_b = \tau \left(\frac{T_s - T_\gamma}{1+z} \right)$$



Line-of-Sight Anisotropy of 21cm Flux Fluctuations

$$T_b = \tau \left(\frac{T_s - T_\gamma}{1+z} \right)$$

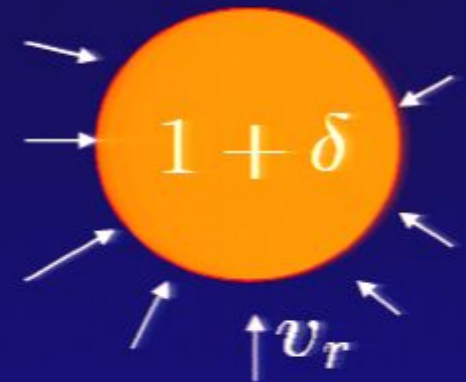
Peculiar velocity changes $\tau \propto \frac{n_{\text{HI}}}{dv_r/dr}$



Line-of-Sight Anisotropy of 21cm Flux Fluctuations

$$T_b = \tau \left(\frac{T_s - T_\gamma}{1+z} \right)$$

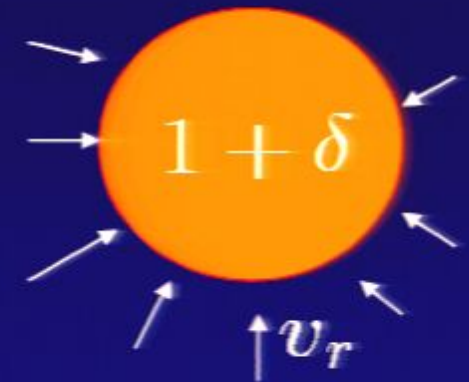
Peculiar velocity changes $\tau \propto \frac{n_{\text{HI}}}{dv_r/dr}$



Line-of-Sight Anisotropy of 21cm Flux Fluctuations

$$T_b = \tau \left(\frac{T_s - T_\gamma}{1+z} \right)$$

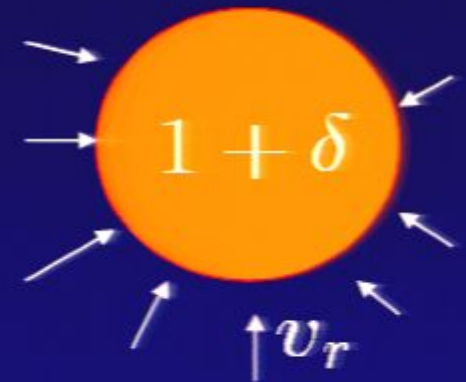
Peculiar velocity changes $\tau \propto \frac{n_{\text{HI}}}{dv_r/dr} = \bar{n}(1+\delta) \sim \bar{H}(1 - \frac{1}{3}\delta)$



Line-of-Sight Anisotropy of 21cm Flux Fluctuations

$$T_b = \tau \left(\frac{T_s - T_\gamma}{1+z} \right)$$

Peculiar velocity changes $\tau \propto \frac{n_{\text{HI}}}{dv_r/dr} = \bar{n}(1+\delta) \sim \bar{H}(1 - \frac{1}{3}\delta)$



→ Power spectrum is not isotropic (“Kaiser effect”)

Line-of-Sight Anisotropy of 21cm Flux Fluctuations

$$T_b = \tau \left(\frac{T_s - T_\gamma}{1+z} \right)$$

Peculiar velocity changes $\tau \propto \frac{n_{\text{HI}}}{dv_r/dr} = \bar{n}(1+\delta) \sim \bar{H}(1 - \frac{1}{3}\delta)$

→ *Power spectrum is not isotropic* (“Kaiser effect”)



Line-of-Sight Anisotropy of 21cm Flux Fluctuations

$$T_b = \tau \left(\frac{T_s - T_\gamma}{1+z} \right)$$

Peculiar velocity changes $\tau \propto \frac{n_{\text{HI}}}{dv_r/dr} = \bar{n}(1+\delta) \sim \bar{H}(1 - \frac{1}{3}\delta)$

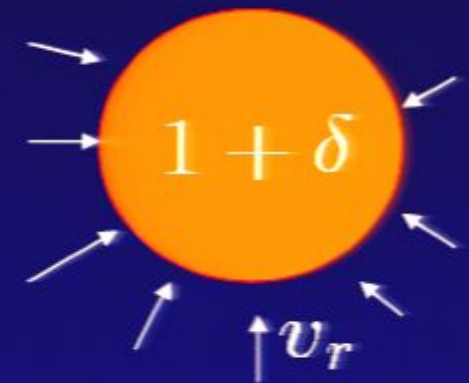
→ *Power spectrum is not isotropic* (“Kaiser effect”)



Line-of-Sight Anisotropy of 21cm Flux Fluctuations

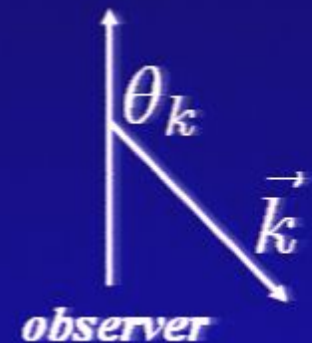
$$T_b = \tau \left(\frac{T_s - T_\gamma}{1+z} \right)$$

Peculiar velocity changes $\tau \propto \frac{n_{\text{HI}}}{dv_r/dr} = \bar{n}(1+\delta) \sim \bar{H}(1 - \frac{1}{3}\delta)$



\rightarrow *Power spectrum is not isotropic ("Kaiser effect")*

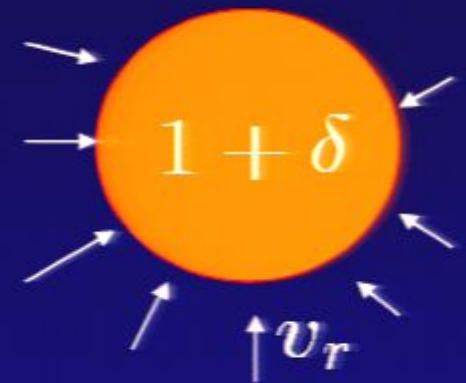
$$\frac{dv_r}{dr} \rightarrow \delta_v(\vec{k}) = -\cos^2 \theta_k \times \delta(\vec{k})$$



Line-of-Sight Anisotropy of 21cm Flux Fluctuations

$$T_b = \tau \left(\frac{T_s - T_\gamma}{1+z} \right)$$

Peculiar velocity changes $\tau \propto \frac{n_{\text{HI}}}{dv_r/dr} = \bar{n}(1+\delta) \sim \bar{H}(1 - \frac{1}{3}\delta)$



→ *Power spectrum is not isotropic* (“Kaiser effect”)

$$\frac{dv_r}{dr} \rightarrow \delta_v(\vec{k}) = -\cos^2 \theta_k \times \delta(\vec{k})$$

$$P_{T_b} = [\cos^2 \theta_k \delta(\vec{k}) + \delta_{\text{iso}}(\vec{k})]^2$$



Line-of-Sight Anisotropy of 21cm Flux Fluctuations

$$T_b = \tau \left(\frac{T_s - T_\gamma}{1+z} \right)$$

Peculiar velocity changes $\tau \propto \frac{n_{\text{HI}}}{dv_r/dr} = \bar{n}(1+\delta) \sim \bar{H}(1 - \frac{1}{3}\delta)$

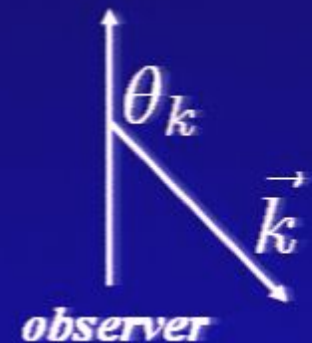


→ *Power spectrum is not isotropic* (“Kaiser effect”)

$$\frac{dv_r}{dr} \rightarrow \delta_v(\vec{k}) = -\cos^2 \theta_k \times \delta(\vec{k})$$

$$P_{T_b} = [\cos^2 \theta_k \delta(\vec{k}) + \delta_{\text{iso}}(\vec{k})]^2$$

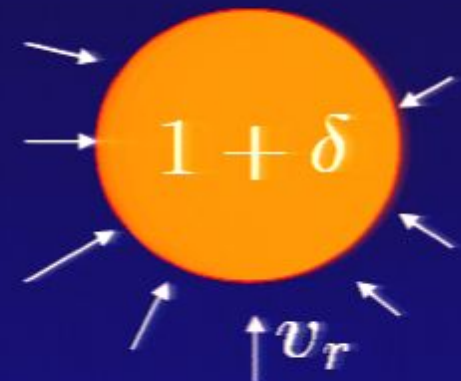
$$\delta_{\text{iso}} = \beta\delta + \delta_{x_{\text{HI}}} + \delta_T + \dots$$



Line-of-Sight Anisotropy of 21cm Flux Fluctuations

$$T_b = \tau \left(\frac{T_s - T_\gamma}{1+z} \right)$$

Peculiar velocity changes $\tau \propto \frac{n_{\text{HI}}}{dv_r/dr} = \bar{n}(1+\delta) \sim \bar{H}(1 - \frac{1}{3}\delta)$



→ *Power spectrum is not isotropic* (“Kaiser effect”)

$$\frac{dv_r}{dr} \rightarrow \delta_v(\vec{k}) = -\cos^2 \theta_k \times \delta(\vec{k})$$

$$P_{T_b} = [\cos^2 \theta_k \delta(\vec{k}) + \delta_{\text{iso}}(\vec{k})]^2$$

$$\delta_{\text{iso}} = \beta\delta + \delta_{x_{\text{HI}}} + \delta_T + \dots$$

$$\cos^4 \theta_k, \cos^2 \theta_k, \cos^0 \theta_k$$



Line-of-Sight Anisotropy of 21cm Flux Fluctuations

$$T_b = \tau \left(\frac{T_s - T_\gamma}{1+z} \right)$$

Peculiar velocity changes $\tau \propto \frac{n_{\text{HI}}}{dv_r/dr} = \bar{n}(1+\delta) \sim \bar{H}(1 - \frac{1}{3}\delta)$



\rightarrow *Power spectrum is not isotropic ("Kaiser effect")*

$$\frac{dv_r}{dr} \rightarrow \delta_v(\vec{k}) = -\cos^2 \theta_k \times \delta(\vec{k})$$



$$P_{T_b} = [\cos^2 \theta_k \delta(\vec{k}) + \delta_{\text{iso}}(\vec{k})]^2$$

$$\delta_{\text{iso}} = \beta\delta + \delta_{x_{\text{HI}}} + \delta_T + \dots$$

$\cos^4 \theta_k, \cos^2 \theta_k, \cos^0 \theta_k$ *terms allow separation of powers*

Experiments

**MWA (Murchison Wide-Field Array)*

MIT/U. Melbourne, ATNF, ANU/CfA/Raman I.

**LOFAR (Low-frequency Array)*

Netherlands

**21CMA (formerly known as PAST)*

China

**PAPER*

UCB/NRAO

**GMRT (Giant Meterwave Radio Telescope)*

India/CITA/Pittsburg

**SKA (Square Kilometer Array)*

International



Murchison Wide-Field Array: mapping cosmic hydrogen through its 21cm emission



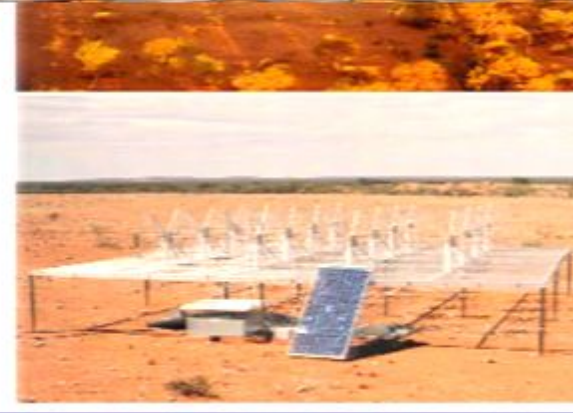
- 4mx4m tiles of 16 dipole antennae, 80-300MHz
- 500 antenna tiles with total collecting area 8000 sq.m. at 150MHz across a 1.5km area: few arcmin resolution

Murchison Wide-Field Array: mapping cosmic hydrogen through its 21cm emission



- 4mx4m tiles of 16 dipole antennae, 80-300MHz
- 500 antenna tiles with total collecting area 8000 sq.m. at 150MHz across a 1.5km area: few arcmin resolution

Murchison Wide-Field Array: mapping cosmic hydrogen through its 21cm emission



- 4mx4m tiles of 16 dipole antennae, 80-300MHz
- 500 antenna tiles with total collecting area 8000 sq.m. at 150MHz across a 1.5km area: few arcmin resolution

Primary challenge: foregrounds

Primary challenge: foregrounds

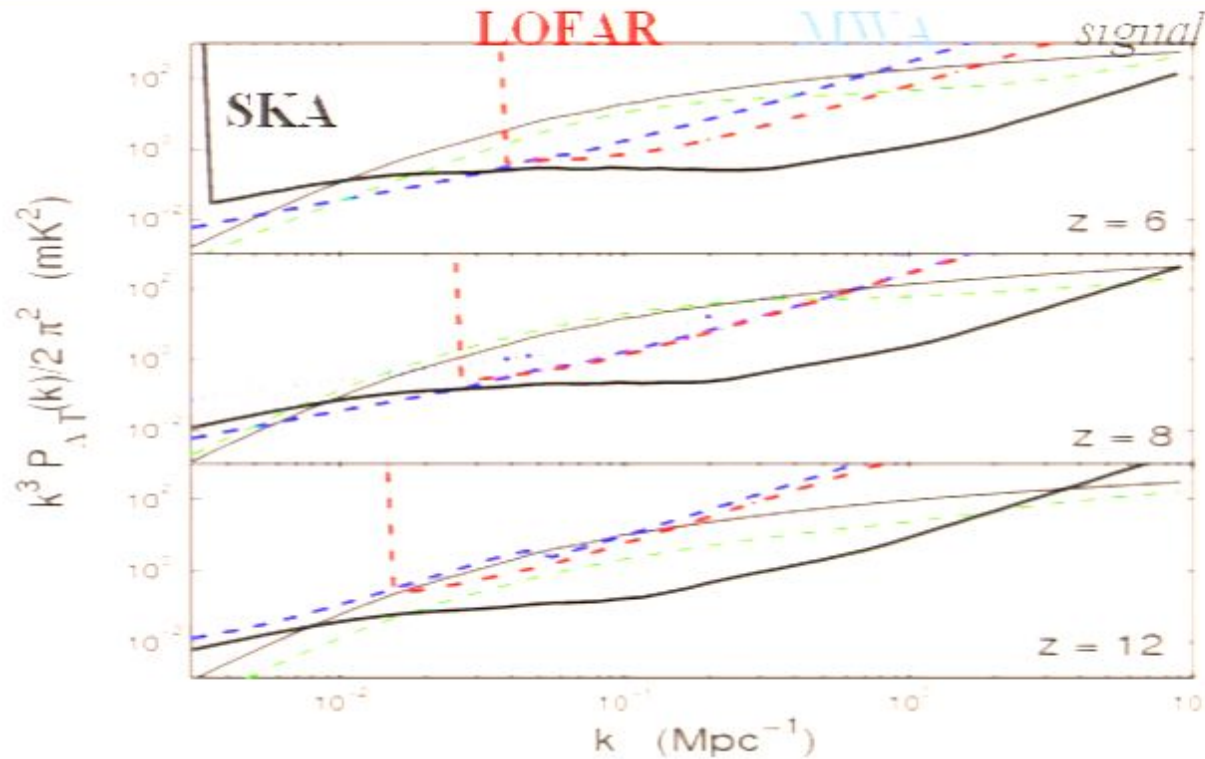
- Terrestrial: radio broadcasting
- Galactic synchrotron emission

Primary challenge: foregrounds

- Terrestrial: radio broadcasting
- Galactic synchrotron emission
- Extragalactic: radio sources

Although the sky brightness ($>10\text{K}$) is much larger than the 21cm signal ($<10\text{mK}$), the foregrounds have a smooth frequency dependence while the signal fluctuates rapidly across small shifts in frequency ($=\text{redshift}$). Theoretical estimates indicate that the 21cm signal is detectable with the forthcoming generation of low-frequency arrays (Zaldarriaga et al. astro-ph/0311514; Morales & Hewitt astro-ph/0312437)

Power-Spectrum Sensitivity



Isotropic power spectrum sensitivity, in logarithmic bins with $\Delta k = k/2$, for several experimental configurations. In each panel, the thin solid and dashed curves show estimates of the signal with and without reionization. The thick solid, dashed, and dot-dashed curves show error estimates for 1000 hour observations over 6 MHz with the SKA, MWA, and LOFAR, respectively. Each assumes perfect foreground removal. The dotted curve in the middle panel assumes a flat antenna distribution for the MWA. From

McQuinn et al. 2006

$$T_{\text{sky}} \sim 180 \left(\frac{\nu}{180 \text{ MHz}} \right)^{-2.6} \text{ K}$$

$$\Delta T^N|_{\text{int}} \sim 2 \text{ mK} \left(\frac{A_{\text{tot}}}{10^5 \text{ m}^2} \right)^{-1} \left(\frac{10'}{\Delta\theta} \right)^2 \left(\frac{1+z}{10} \right)^{4.6} \left(\frac{\text{MHz}}{\Delta\nu} \frac{100 \text{ hr}}{t_{\text{int}}} \right)^{1/2}$$

21cm Cosmology After Reionization?

21cm Cosmology After Reionization?

Damped Ly α absorbers:

21cm Cosmology After Reionization?

Damped Ly α absorbers: $\Omega_{\text{DLA}} \sim 10^{-3}$

$$f_{\text{HI}} = (\Omega_{\text{DLA}}/\Omega_b) \approx 3\%, \text{ at } : z < 6$$

21cm Cosmology After Reionization?

Damped Ly α absorbers: $\Omega_{\text{DLA}} \sim 10^{-3}$

$$f_{\text{HI}} = (\Omega_{\text{DLA}}/\Omega_b) \approx 3\%, \text{ at } z < 6$$

$$\sigma_8 \sim 0.2, \text{ at } z \sim 4$$

21cm Cosmology After Reionization?

Damped Ly α absorbers: $\Omega_{\text{DLA}} \sim 10^{-3}$

$$f_{\text{HI}} = (\Omega_{\text{DLA}}/\Omega_b) \approx 3\%, \text{ at } : z < 6$$

$$\sigma_8 \sim 0.2, \text{ at } : z \sim 4 \rightarrow (\delta T)_{\text{signal}} \sim 0.1\text{mK} \quad \text{on } 10\text{cMpc}$$

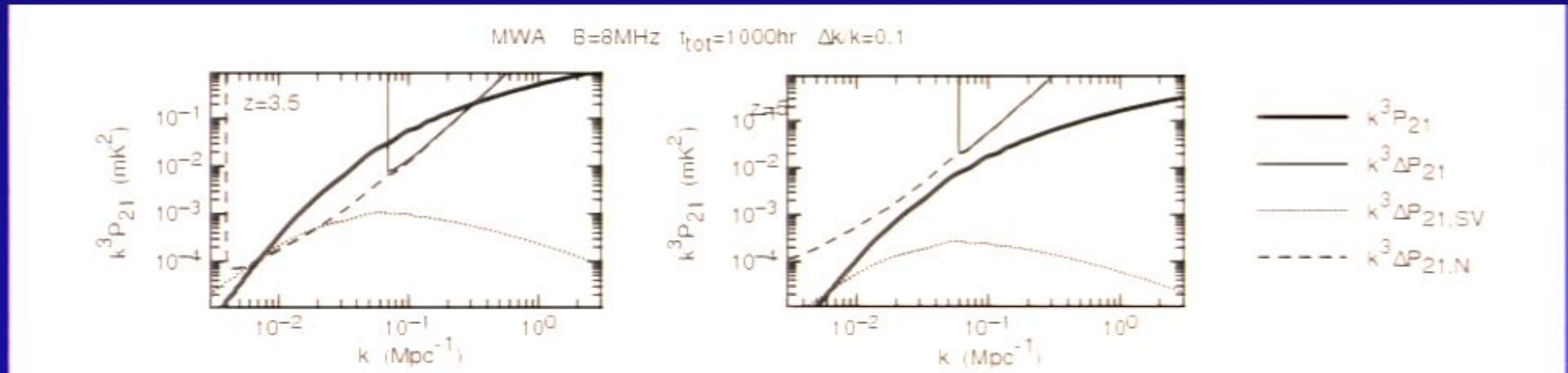
21cm Cosmology After Reionization?

Damped Ly α absorbers: $\Omega_{\text{DLA}} \sim 10^{-3}$

$$f_{\text{HI}} = (\Omega_{\text{DLA}}/\Omega_b) \approx 3\%, \text{ at } : z < 6$$

$$\sigma_8 \sim 0.2, \text{ at } : z \sim 4 \rightarrow (\delta T)_{\text{signal}} \sim 0.1 \text{mK} \quad \text{on } 10 \text{cMpc}$$

$$(\delta T)_{\text{noise}} \propto (1+z)^{2.6}$$

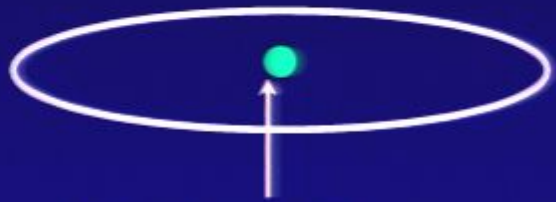


Acoustic Oscillations

Acoustic Oscillations

Inflation: $t=0$

Acoustic Oscillations



Inflation: $t=0$

Acoustic Oscillations



Acoustic Oscillations



Gas is freed to fall into dark matter potential fluctuations at $z \sim 1000$

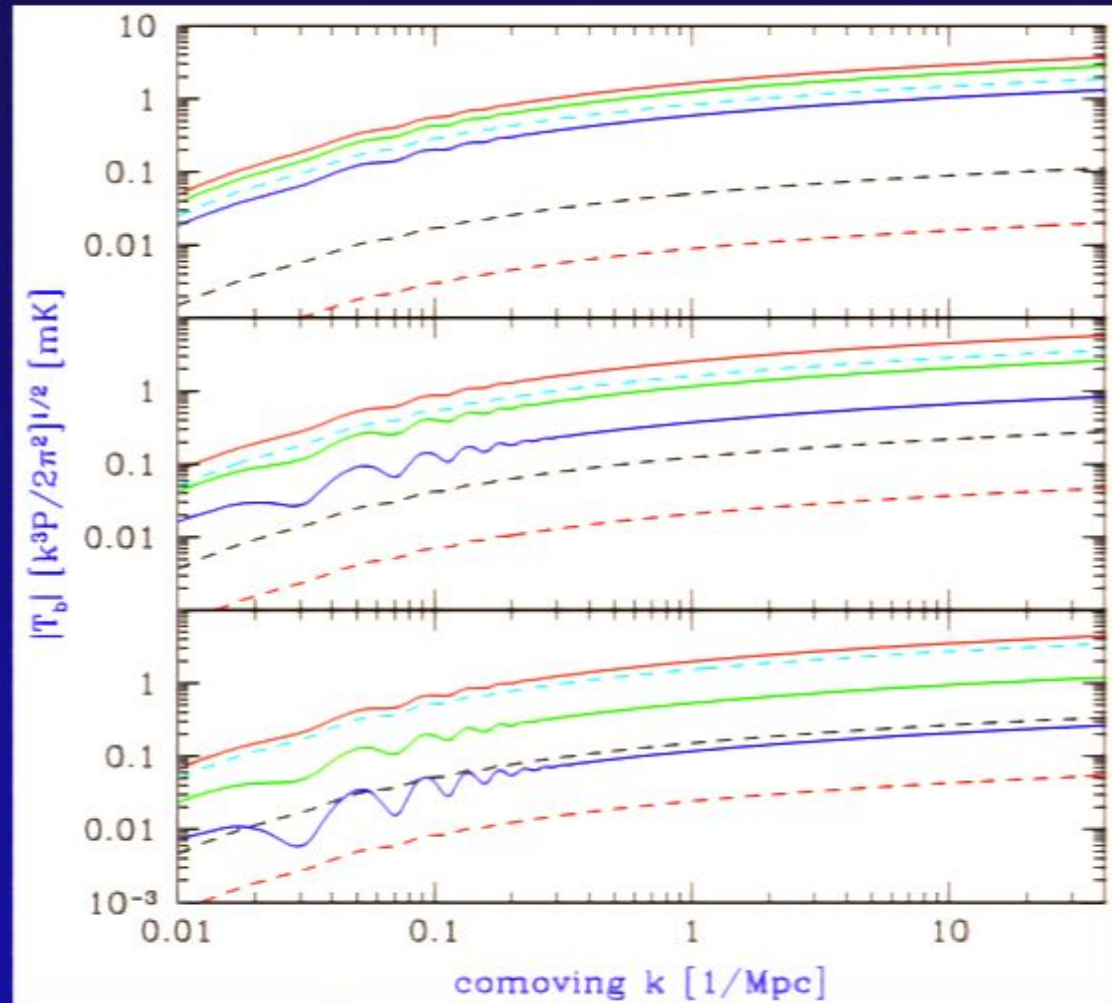
- Correlation across the radiation sound horizon, left over from coupling of gas to CMB at $z > 1000$.*
- Standard ruler- sensitive probe to contribution from dark energy at redshifts $0 < z < 200$*

Acoustic Oscillations



Inflation: $t=0$

Gas is freed to fall into dark matter potential fluctuations at $z \sim 1000$



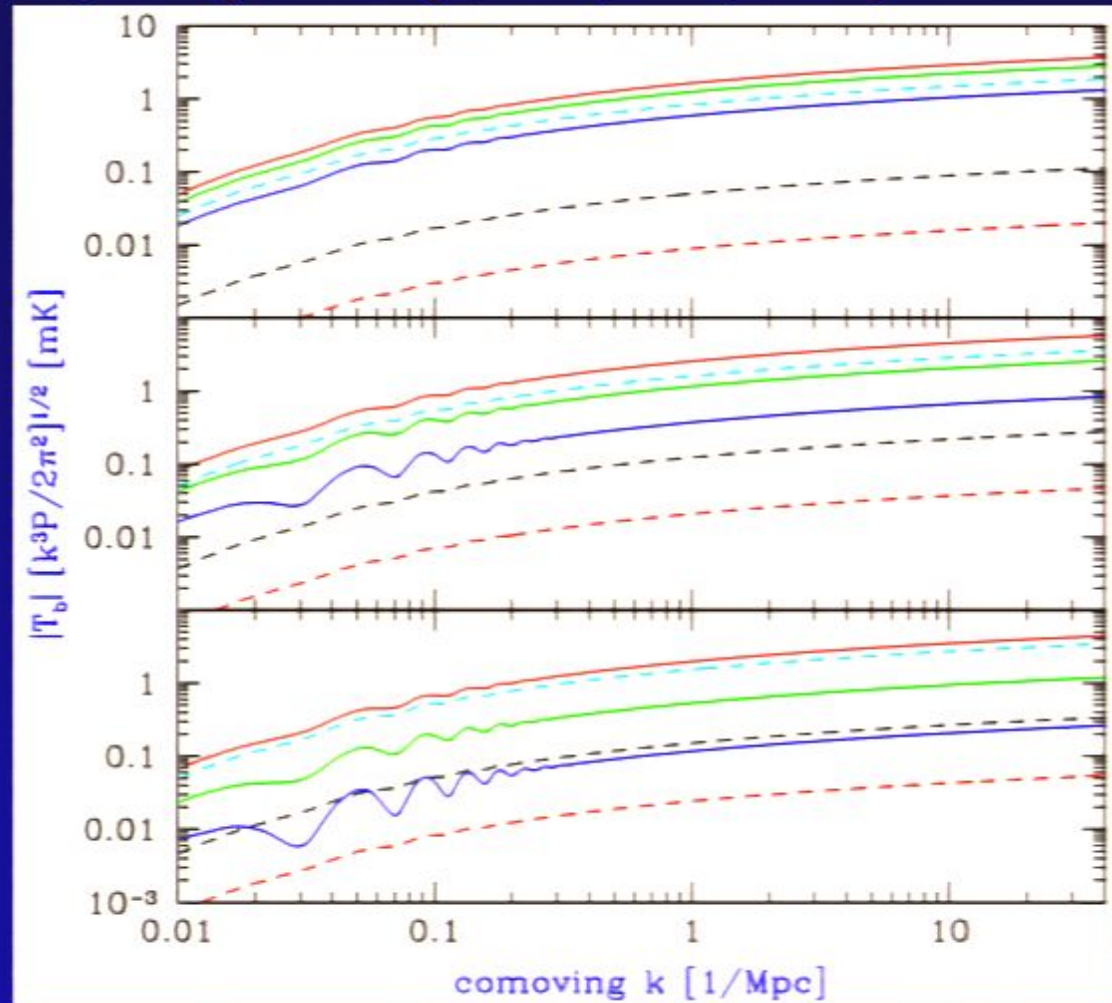
- *Correlation across the radiation sound horizon, left over from coupling of gas to CMB at $z > 1000$.*
- *Standard ruler- sensitive probe to contribution from dark energy at redshifts 0.200*

Acoustic Oscillations

$z = 150, 100, 30$ (solid); $35, 20, 15$ (dashed)

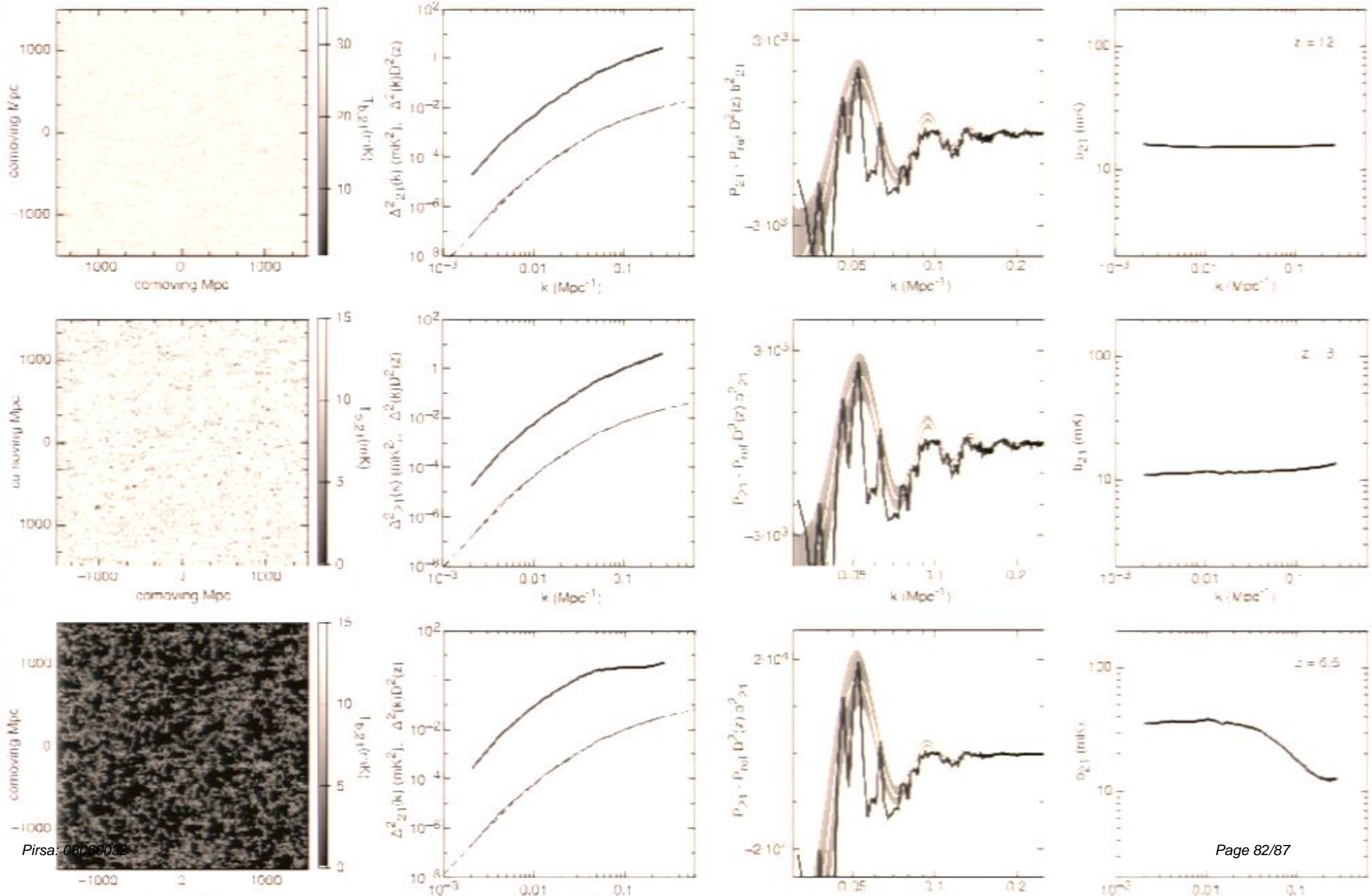


Gas is freed to fall into dark matter potential fluctuations at $z \sim 1000$



- Correlation across the radiation sound horizon, left over from coupling of gas to CMB at $z > 1000$.
- Standard ruler - sensitive probe to contribution from dark energy at redshifts 0.200

Acoustic Oscillations



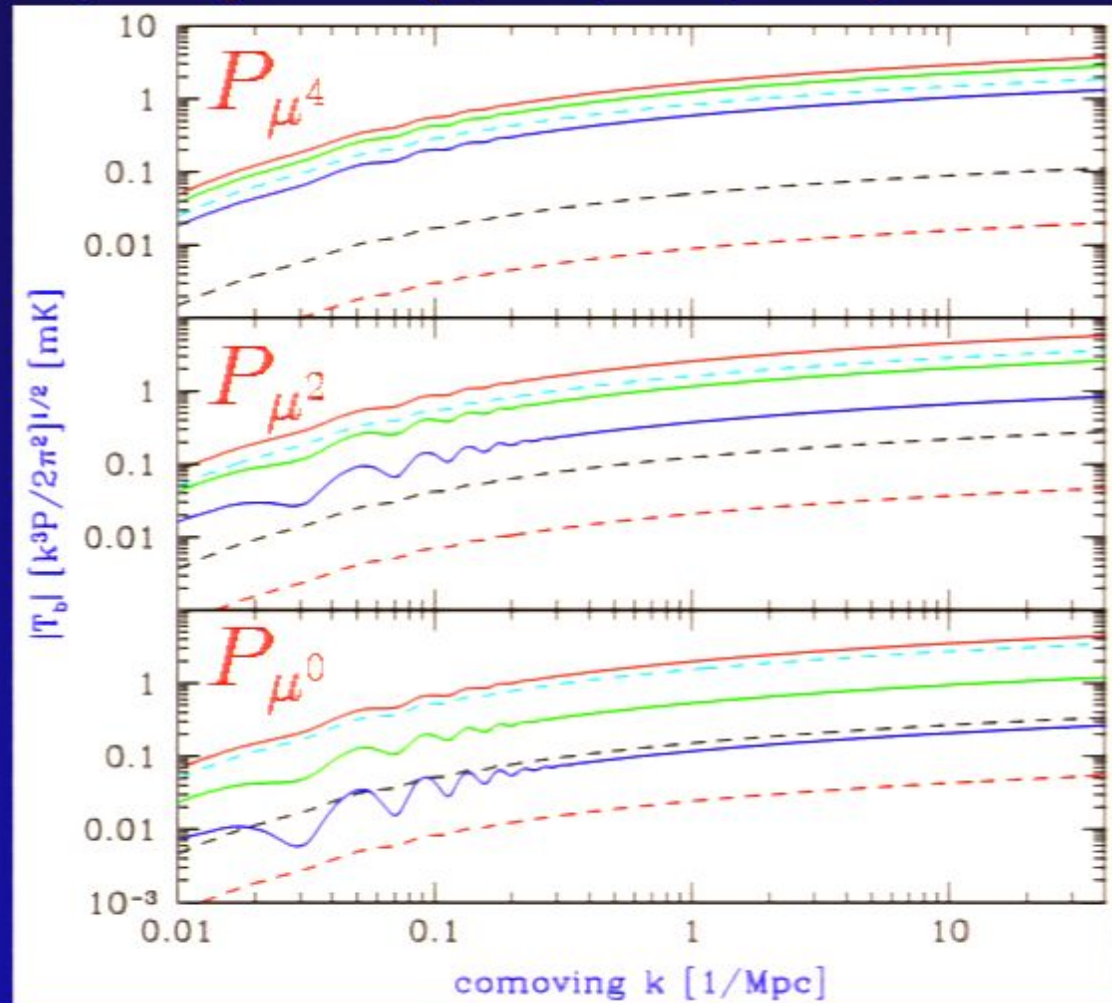
Acoustic Oscillations

$z = 150, 100, 30$ (solid); $35, 20, 15$ (dashed)



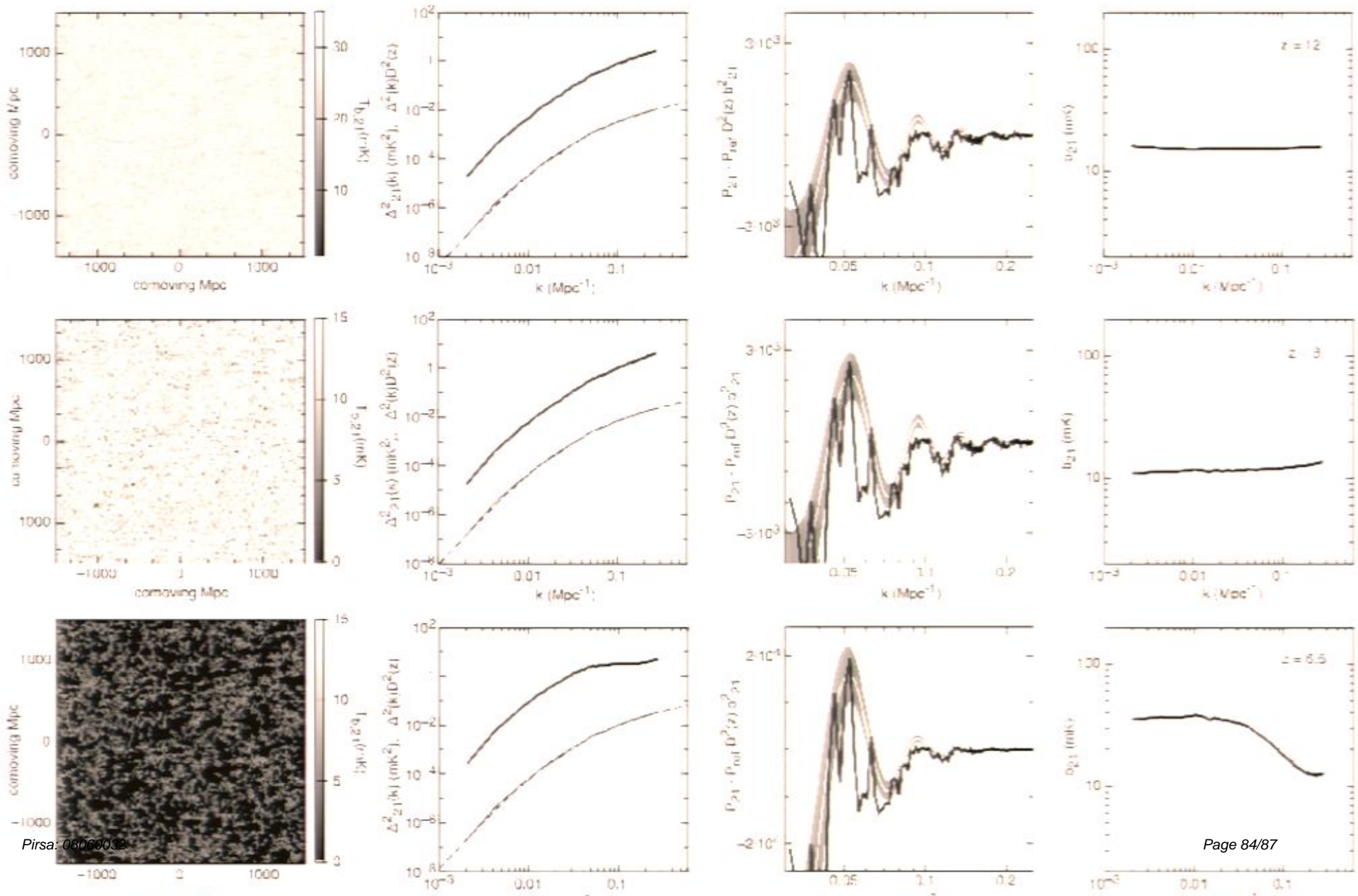
Inflation: $t=0$

Gas is freed to fall into dark matter potential fluctuations at $z \sim 1000$



- Correlation across the radiation sound horizon, left over from coupling of gas to CMB at $z > 1000$.
- Standard ruler- sensitive probe to contribution from dark energy at redshifts 0-200

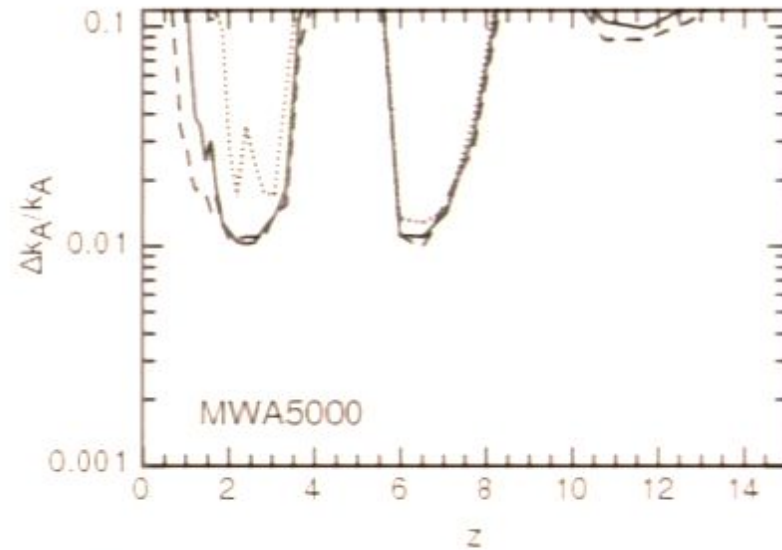
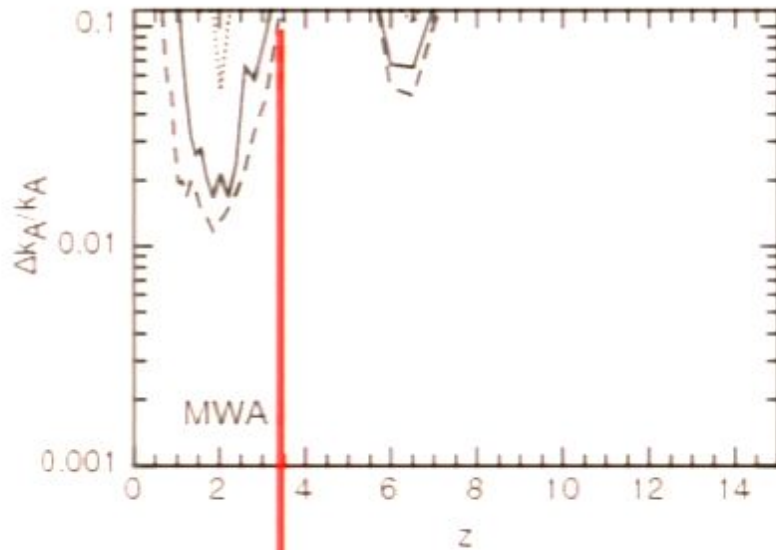
Acoustic Oscillations



Acoustic Oscillations

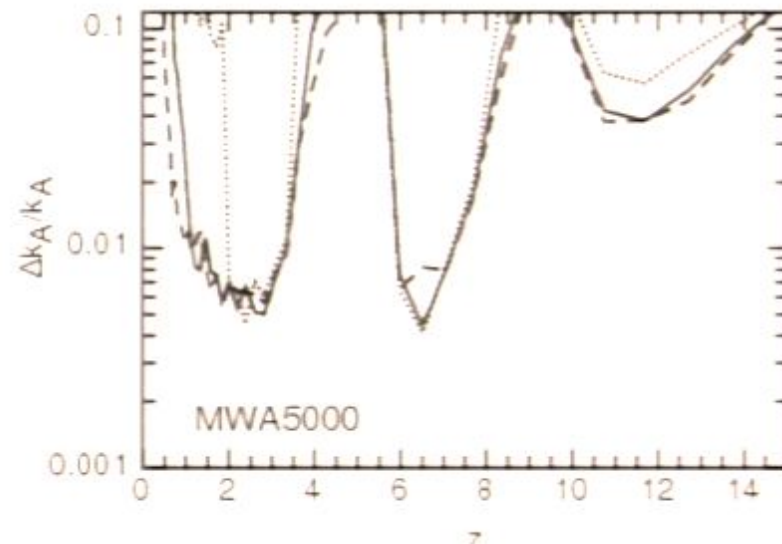
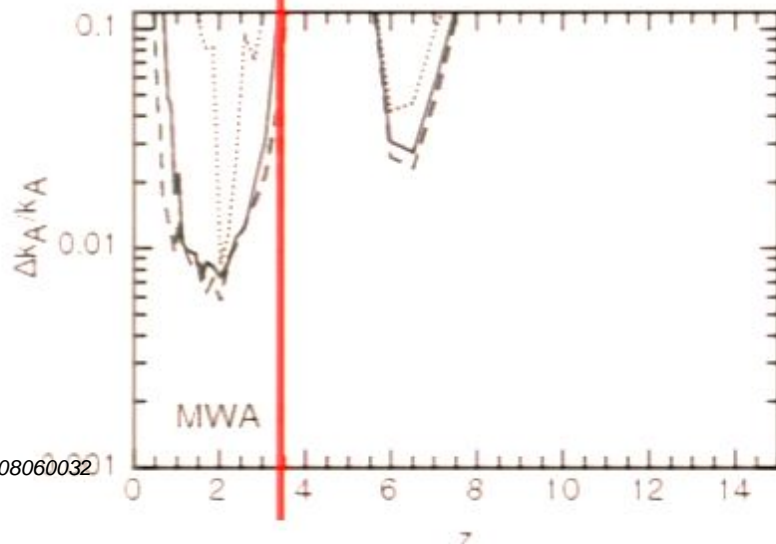
Vyithe, Loeb & Geil

1 field x 1000 hrs



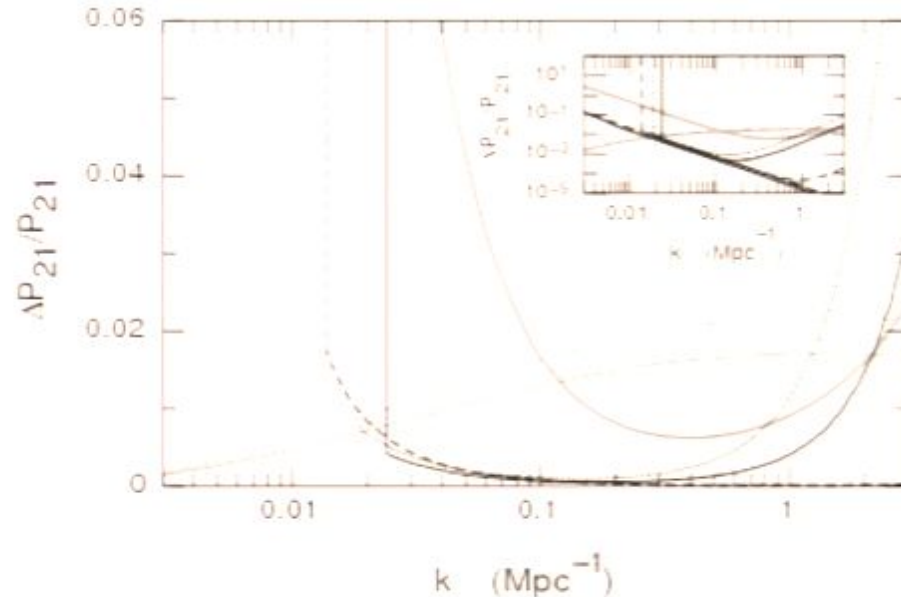
..... 6 MHz
—— 8 MHz
- - - 12 MHz

3 fields x 1000 hrs



..... 6 MHz
—— 8 MHz
- - - 12 MHz

Weighting Neutrinos with a 21cm Survey at $z < 6$



The fractional change in the amplitude of the power-spectrum owing to the presence of a massive neutrino (horizontal grey lines, asymptoting towards a constant at high k values). The case shown, $f_\nu = 0.004$, corresponds to $m_\nu = 0.05\text{eV}$. For comparison, the limits imposed by cosmic variance on the *SDSS*-LRG measurements of the power-spectrum are marked by the thick grey line. The U -shaped error curves correspond to an all-sky 21cm survey [$f_{\text{sky}} = 0.65$ over a redshift range spanning a factor of 3 in $(1+z)$] with MWA5000 and a 10^3 hour integration per field (line styles for $z = 1.5, 3.5, 6.5$ as in Figure 2). The inset shows these results on logarithmic axes that span a larger dynamic range of achievable precision. The straight thin lines in the inset show the cosmic-variance uncertainty in the power-spectrum

Loeb & Wyithe,
PRL, in press

Page 86/87

Highlights

- *Redshifted 21cm from $0 < z < 200$ can be used to map the matter distribution throughout most of the comoving volume of the observable universe*
- *Dark energy can be constrained through baryonic acoustic oscillations in the 21cm power-spectrum*
- *Neutrino mass can be detected at the level expected from atmospheric neutrino data (0.05eV).*
- *Alternative models of gravity can be constrained by measuring the growth of structure at moderate redshifts that cannot be accessed by other means*